Available online at www.sciencedirect.com
ScienceDirect
Journal of Power Sources 165 (2007) 739–756
JOURNAL OF POWER SOURCES
www.elsevier.com/locate/jpowsour

Review

A review of PEM hydrogen fuel cell contamination: Impacts, mechanisms, and mitigation

Xuan Cheng [a,b], Zheng Shi [a], Nancy Glass [a], Lu Zhang [b], Jiujun Zhang [a,*], Datong Song [a], Zhong-Sheng Liu [a], Haijiang Wang [a], Jun Shen [a]

[a] *Institute for Fuel Cell Innovation, National Research Council of Canada, Vancouver, BC V6T 1W5, Canada*
[b] *Department of Materials Science and Engineering, State Key Laboratory for Physical Chemistry of Solid Surfaces, Xiamen University, Xiamen, FJ 361005, PR China*

Received 15 November 2006; received in revised form 9 December 2006; accepted 11 December 2006
Available online 8 January 2007

Abstract

This paper reviewed over 150 articles on the subject of the effect of contamination on PEM fuel cell. The contaminants included were fuel impurities (CO, CO_2, H_2S, and NH_3); air pollutants (NO_x, SO_x, CO, and CO_2); and cationic ions Fe^{3+} and Cu^{2+} resulting from the corrosion of fuel cell stack system components. It was found that even trace amounts of impurities present in either fuel or air streams or fuel cell system components could severely poison the anode, membrane, and cathode, particularly at low-temperature operation, which resulted in dramatic performance drop. Significant progress has been made in identifying fuel cell contamination sources and understanding the effect of contaminants on performance through experimental, theoretical/modeling, and methodological approaches. Contamination affects three major elements of fuel cell performance: electrode kinetics, conductivity, and mass transfer.

This review was focused on three areas: (1) contamination impacts on the fuel cell performance, (2) mechanism approaches dominated by modeling studies, and (3) mitigation development. Some future work on fuel cell contamination research is suggested in order to facilitate the move toward commercialization.

Keywords: PEM fuel cells; Contamination; Mechanism; Modeling; Pt catalyst poisoning; Fuel impurities and air pollutants

Contents

* Corresponding author. Tel.: +1 604 221 3087; fax: +1 604 221 3001.
E-mail address: jiujun.zhang@nrc.gc.ca (J. Zhang).

0378-7753/$ – see front matter © 2006 Elsevier B.V. All rights reserved.
doi:10.1016/j.jpowsour.2006.12.012

1. Introduction

Fuel cells are considered to be the green power sources for the 21st century, and may make the "hydrogen economy" a reality. The main driving force for fuel cell research, development, and commercialization is the increasing concern about global pollution caused by energy emissions, especially from transportation and stationary applications [1,2]. The biggest advantage of proton exchange membrane fuel cells (PEMFCs) over internal combustion engines in automotive vehicles is the fact that PEMFCs produce zero emissions when using hydrogen as the fuel and air as the oxidant. With respect to other high power-demanding areas such as residential and electronic applications, PEMFCs also have advantages in terms of power density and efficiency [3,4].

However, impurities in hydrogen fuel, such as CO, H_2S, NH_3, organic sulfur–carbon, and carbon–hydrogen compounds, and in air, such as NO_x, SO_x, and small organics, are brought along with the fuel and air feed streams into the anodes and cathodes of a PEMFC stack, causing performance degradation, and sometimes permanent damage to the membrane electrode assemblies (MEAs) [5,6]. The hydrogen impurities mentioned above are mainly from the manufacturing process, in which natural gas (CH_4) or other small organic fuels are re-formed to produce hydrogen gas with a small amount of impurities. The air pollutants are mainly from vehicle exhaust and industrial emissions. Some undesired metal ions such as Fe^{3+} and Cu^{2+}, as well as greases, coming from the system components are also harmful to the MEAs [7]. These effects of all of the above impurities are referred to as fuel cell contamination [8].

The effect of contaminants on fuel cells is one of the most important issues in fuel cell operation and applications [8]. At the current stage of research into fuel cell contamination, three major areas have been addressed: (1) theoretical and empirical modeling of contamination to provide a fundamental understanding of the mechanisms, (2) experimental observation and validation, and (3) mitigation of the effects of contaminants. In recent years, work toward identifying the potential impacts of contamination, understanding the contamination mechanisms, and developing mitigation strategies has drawn a great deal of attention to fuel cells and their applications in the automobile industry.

With respect to applications, the technical reports prepared by Park and O'Brien [5] and Hayter et al. [6] briefly reviewed the effects of contaminants in the fuel and air steams on cell performance. They discussed CO, CO_2, NH_3, H_2S, and inert diluents such as N_2 with respect to anode contamination; SO_x and NO_x (cathode contamination); and NH_3 and metallic species leached from the cell components (membrane contamination). Since then, a considerable amount of work has been carried out which focuses on the impacts of contaminants on fuel cell performance and lifetime, which will be comprehensively reviewed in this article.

In terms of fundamental understanding, it has been identified that the fuel cell component most affected by a contamination process is the membrane electrode assembly (MEA). Three major effects have been identified [9]: (1) kinetic effect (poisoning of the electrode catalysts), (2) conductivity effect (increase in the solid electrolyte resistance, including that of the membrane and catalyst layer ionomer), and (3) mass transfer effect (catalyst layer structure and hydrophobility changes causing a mass transfer problem).

In general, most of the published work has focused on the influence of individual and particular contaminants on PEMFCs. A general overview covering every aspect of fuel cell contamination has not yet appeared in the literature. Therefore, it is necessary to obtain updated and detailed information that is as broad as possible in order to identify the problems and to gain knowledge and fundamental understanding of contamination mechanisms. Then, based on validated mechanisms, effective control strategies can be developed to improve the reliability and durability of PEMFCs in order to accelerate the commercialization process of fuel cell technology.

In this paper, the nature and sources of contaminants, their impacts on fuel cell performance and lifetime, and the poisoning mechanisms of contamination are reviewed in a broad scope. The major findings from both experimental and theoretical studies in

contamination-related research are summarized. The methods or tools developed to diagnose various contamination phenomena are introduced. Accordingly, the existing strategies to mitigate the adverse effects of contamination are also briefly mentioned. In addition, key issues in the future R&D of fuel cell contamination and control are discussed. Due to the limited the length of this review, only hydrogen fuels will be discussed here because of their importance in practical PEM fuel cell applications.

2. Contamination sources

2.1. Fuel (hydrogen) contamination sources

At the current stage of technology, the hydrogen used as a direct fuel in fuel cell research, development, and demonstration comes mainly from commercially available sources and on-board production. The reformation of hydrocarbons and/or oxygenated hydrocarbons including methane from natural gases [10] and methanol from biomass [11,12] is the dominant method for hydrogen production, among others such as electrolysis, partial oxidation (or autothermal reforming) of small organics [13], and hydrolysis of sodium borohydride [14]. However, the reformation process of hydrogen production results in unavoidable impurities such as carbon oxides including CO and CO_2, and sulfur compounds including H_2S and sulfur organics. Steam reforming and partial oxidation or autothermal reforming are usually used to produce hydrogen-rich gas called "reformate," which typically contains 40 to 70% H_2, 15 to 25% CO_2, 1 to 2% CO, small quantities of inert gases (water vapor and nitrogen), and sulfur impurities. On the other hand, the use of ammonia as a tracer gas in natural gas distribution systems can result in NH_3 impurity (at a level of few ppm) in the reformate gas. With respect to high performance and long lifetime, purer hydrogen is required for the fuel cell feed. The separation processes to remove undesired impurities in the reformate gas are necessary but costly. For trace levels of CO and sulfur compounds, filtration seems even more difficult and expensive.

2.2. Air contamination sources

Air is the most practical and economical way to feed the fuel cell stack. However, air pollutants, namely nitrogen oxides (NO_x, including NO and NO_2), sulfur oxides (SO_x, including SO_2 and SO_3), carbon oxides (CO_x, including CO and CO_2), ozone, and other organic chemical species (such as benzoic compounds) contaminate the fuel cell, resulting in MEA damage and performance degradation [15–17]. The major sources of these contaminants are the automotive vehicle exhaust and industrial manufacturing processes. For example, the NO_x level in the Vancouver BC can be as high as 100 ppb, which could cause an approximate 25 mV voltage drop in single fuel cell performance, as shown in Fig. 1 [9]. In a battlefield, the SO_x could be as high as 0.5 ppm, which could cause a power failure in a fuel cell stack power supply [15], because the MEA in current PEM fuel cell stacks operating at low temperature (<80 °C) cannot tolerate impurities even at levels as low as ppm.

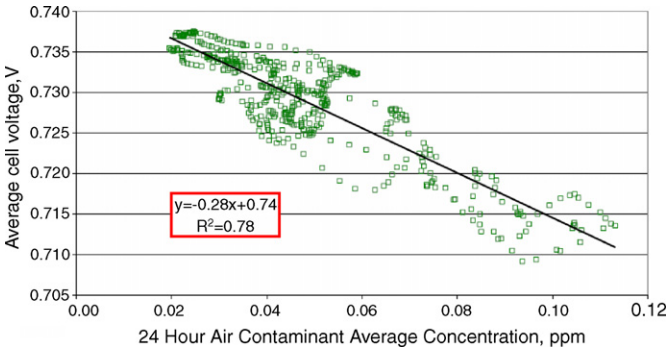

Fig. 1. Average cell voltage as a function of 24 h average NO_x concentration. Air/methane reformate, Nafion 112 pressed with electrodes of total Pt loading of 1.0 mg cm^{-2}, T = 55 °C in/65 °C out, 0.175 A cm^{-2}, 1.28 bar, and air/fuel stoichiometries of 2.00/1.25 [9].

Table 1
Major contaminants identified in the operation of PEM fuel cells

Impurity source	Typical contaminant
Air	N_2, NO_x (NO, NO_2), SO_x (SO_2, SO_3) NH_3, O_3
Reformate hydrogen	CO, CO_2, H_2S, NH_3, CH_4
Bipolar metal plates (end plates)	Fe^{3+}, Ni^{2+}, Cu^{2+}, Cr^{3+}
Membranes (Nafion®)	Na^+, Ca^{2+}
Sealing gasket	Si
Coolants, DI water	Si, Al, S, K, Fe, Cu, Cl, V, Cr
Battlefield pollutants	SO_2, NO_2, CO, propane, benzene
Compressors	Oils

2.3. Other contamination sources

In addition to the fuel and air contaminants mentioned above, some trace amounts of metallic ions from corrosion of stack or system components, such as flow field bipolar plates, seals, inlet/outlet manifolds, humidifier reservoirs, and cooling loops, or from the fuel or oxidant, membranes, or coolants can also cause fuel cell contamination. Other impurities such as silicon which has dissolved from the sealing gasket [18] have also been reported to have a contaminating effect on fuel cell performance.

Table 1 provides a list of contaminants presented in the operation of PEM fuel cells. This list may not be complete, as suggested by the US Fuel Cell Council [19]. However, it represents the majority of the contaminants identified in fuel cell operations.

3. Contamination impacts

In order to facilitate this discussion, a schematic structure of a PEM fuel cell is presented in Fig. 2. The MEA, the most important component, contains both anode and cathode catalyst layers (CLs), gas diffusion layers (GDLs), and a proton exchange membrane (PEM). Fuel cell contamination refers to any effect that can cause MEA performance degradation.

For anode and cathode CLs, the impurities from feed gases and system components can directly enter the matrix structure (reaction zone), poisoning the catalyst sites, changing MEA

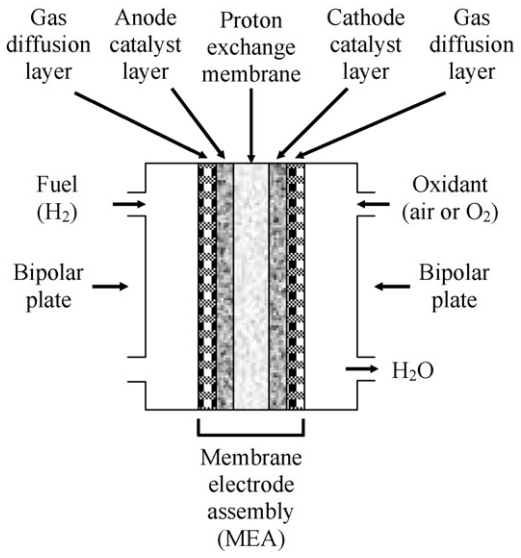

Fig. 2. Basic components of proton exchange membrane fuel cell.

properties such as hydrophobility and hydrophilicity, modifying the proton transportation path, and affecting water management, thus causing performance degradation. The major effect is believed to be the decrease in catalyst activities.

For the PEM, the contaminants – in particular the cations – can get into the membrane to compete with the proton for the $–SO_3^-$ sites (Nafion membrane) and at the same time decrease the water content, resulting in a reduction in proton conductivity. On the other hand, metal ions such as Fe^{3+}/Fe^{2+} inside a membrane can also accelerate membrane degradation during a fuel cell operation through a peroxide formation mechanism [20].

There is little or no literature addressing the effects of contamination on GDLs. It was observed after MEA lifetime testing that GDLs appeared to be less hydrophobic and traces of foreign materials were found on the GDL surface, which were not present before lifetime testing. This could be partially attributed to the contamination effect. The contaminants, including transition metal ions, could become attached or deposited on the carbon fibres, thus changing surface properties such as hydrophobility and hydrophilicity, and resulting in water management or/and mass transfer problems.

In general, the contaminants in Table 1 can cause negative effects on fuel cell performance in different ways. These effects can be categorized into three major types [7,8,20]: (1) kinetic losses due to the poisoning of both anode and cathode electrocatalysts, (2) ohmic losses due to an increase in the resistance of cell components, and (3) mass transport losses due to changes in structure and hydrophobacity of CLs, PEMs, and GDLs.

In the literature, the most extensively investigated contaminants are carbon oxides, particularly CO due to the popularity of H_2 production through a reformate process, which can produce traces of CO and CO_2 in H_2-rich fuel for fuel cell applications. Air stream contaminants such as NO_x and SO_x and trace cationic ions generated from the cell components have also been studied in recent years. In addition, the contamination mechanism and its mitigation, and the implication of contamination for cell degradation and failure has also been studied in recent years.

This section focuses on contamination impacts. The effects of carbon oxides, sulfur-containing species, ammonia, and cationic ions on fuel cell performance are reviewed based on a literature survey. The methods or tools that have been developed to analyze or diagnose CO contamination are also summarized.

3.1. Carbon oxide contamination

3.1.1. Influence of carbon monoxide

Both carbon monoxide and carbon dioxide have become major concerns in PEM fuel cells using reformate H_2-rich gas as fuel, particularly at conventional operating temperatures (<80 °C). It is well documented that CO binds strongly to Pt sites, resulting in the reduction of surface active sites available for hydrogen adsorption and oxidation. With respect to this, Baschuk and Li [21] reviewed the CO poisoning of platinum electrocatalyts used in PEM fuel cells in terms of characteristics, mechanism, mitigation, and theoretical models. It seemed that the CO poisoning effect was strongly related to the concentration of CO, the exposure time to CO, the cell operation temperature, and anode catalyst types.

3.1.1.1. Effects of CO concentration and exposure time. Normally, CO poisoning on Pt electrocatalysts becomes more severe with increases in CO concentration and exposure time. Fig. 3 illustrates typical fuel cell stack polarization curves obtained at 80 °C in both the absence and presence of various concentrations of CO [22,23]. The catalysts used in the stack were pure

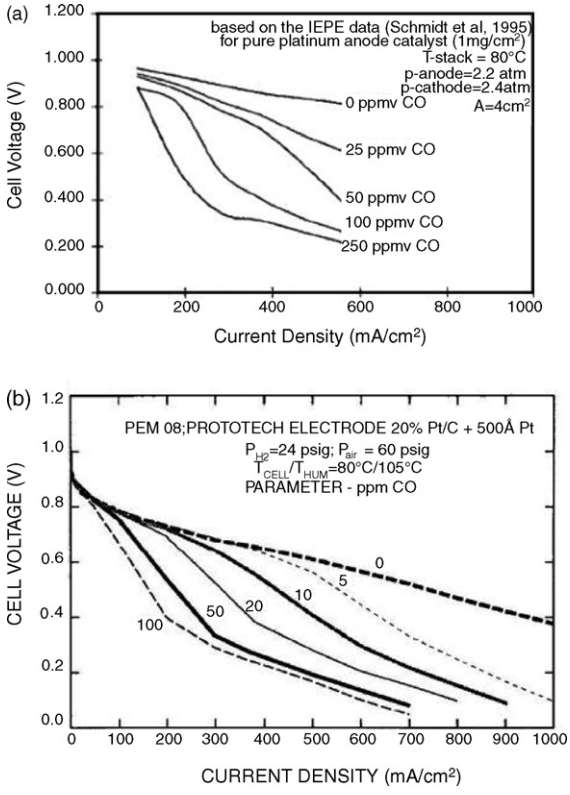

Fig. 3. Effects of CO concentration on cell performance. (a) A stack [22]. (b) A prototech electrode [23].

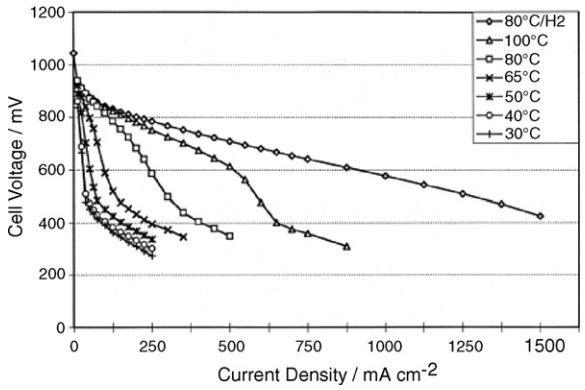

Fig. 4. Temperature dependence of cell performance (30–100 °C, H_2/250 ppm CO). $A = 4\ cm^2$; cathode catalyst: pure Pt; anode catalyst: $Pt_{0.5}Ru_{0.5}$; catalyst loadings: 1 mg cm^{-2}; Nafion® 117 [27].

Pt [22] and carbon-supported Pt [23]. The figure indicates that the CO impurities from fuel streams, even at a level of a few ppm, can cause a substantial degradation in cell performance, especially at high current densities. The voltage losses became deeper with prolonged exposure to CO, due to its accumulation on the Pt catalyst surface over time [12,24]. The voltage loss represented less than 3% at a CO level of 50 ppm after 6 h of exposure. However, an 85% voltage loss was observed when the CO level was increased to 70 ppm [25]. Benesch and Jacksier [26] reported that the time it took for cell voltages to decay to a threshold value of 0.3 V were 1 and 9 h, respectively, when the cells were exposed to 50 and 10 ppm of CO. The cell voltages did not appear to drop below 0.3 V when the CO concentrations were lower than 5 ppm.

3.1.1.2. Effects of operating temperature and pressure. While the severity of catalyst poisoning by CO can be strongly affected by fuel cell operation temperature it may not be sensitive to pressure. At low temperatures (<80 °C), a trace amount of CO can cause a significant performance drop. As shown in Fig. 4, when the anode was fed with H_2 containing 250 ppm of CO, the performance at temperatures below 80 °C was much lower than that at 100 °C [27]. The temperature effect of CO poisoning in the range of 100–200 °C was also studied [28,29]. It was found that higher temperature and higher humidity could effectively reduce CO coverage on the catalyst by promoting CO oxidation with an OH_{ads} group [28]. A PBI membrane-based fuel cell operated at 125, 150, 175 and 200 °C showed a similar trend in the presence of various concentrations of CO in the hydrogen [29]; that is, the higher the temperature, the lower the cell voltage drop.

The combined effects of CO concentration, temperature, and pressure on fuel cell performance at CO concentrations larger than 500 ppm were evaluated as shown in Fig. 5 [30]. As seen in Fig. 5(a), lower temperatures and higher CO concentrations can always cause deeper performance drops. As seen in Fig. 5(b), the pressure effect on cell performance with pure hydrogen is notably different from that with CO-containing hydrogen. The cell performance increased with pure hydrogen when pressure was increased. However, the cell performance was only slightly

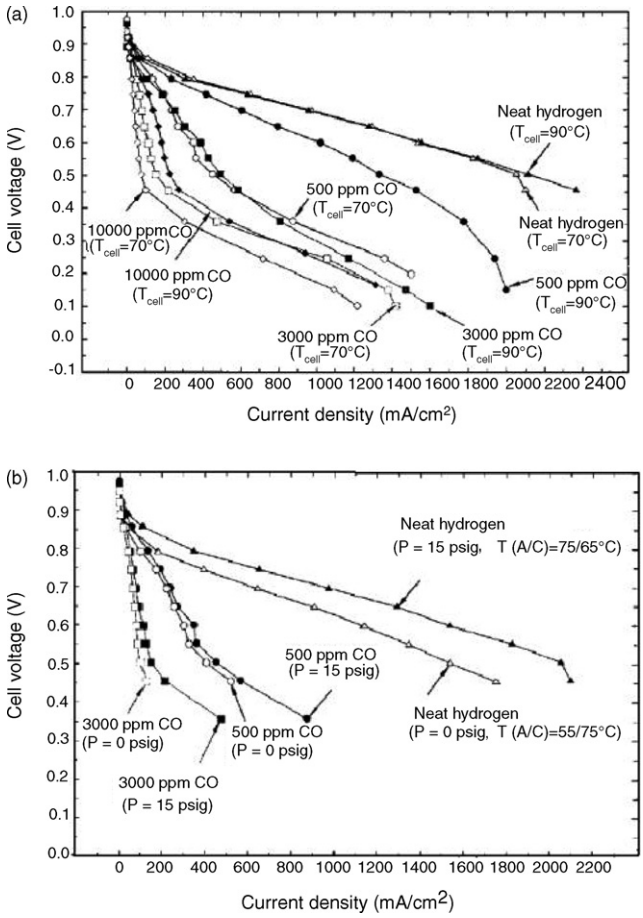

Fig. 5. Effects of temperature and pressure on cell performance at different levels of CO contaminations [30]. $A = 20\ cm^2$; GORE-SELECT® Membrane (25 μm); anode catalyst: Pt alloy at 0.45 mg cm^{-2}; cathode catalyst: Pt at 0.4 mg cm^{-2}. (a) $P = 202$ kPa; (b) $T = 70$ °C.

improved with increasing pressure in the presence of 500 and 3000 ppm CO, particularly at higher current densities.

3.1.1.3. Effects of anode catalyst type. The effects of CO poisoning on pure Pt and Pt-alloy anode catalysts were extensively investigated; a typical example is shown in Fig. 6 [31]. Although both pure Pt and $Pt_{0.5}Ru_{0.5}$ catalysts could be poisoned and the effect could become more severe with increases in CO concentration and exposure time, the cell performance drop for $Pt_{0.5}Ru_{0.5}$ was much shallower than that of pure Pt. For a pure Pt catalyst, two distinct slopes were observed; these could be attributed to the CO adsorption and oxidation kinetics. For a $Pt_{0.5}Ru_{0.5}$ catalyst, only a uniform slope could be seen. This observation suggested a contamination tolerance property of the $Pt_{0.5}Ru_{0.5}$ catalyzed anode. Ralph and Hogarth [32] confirmed that a PtRu alloy catalyst is more tolerant to CO poisoning than a pure Pt electrocatalyst by experiments using a fuel cell operated at 80 °C with hydrogen containing 10, 40, and 100 ppm CO. However, the severity of CO poisoning is also strongly affected by the anode composition, catalyst preparation procedures, fuel cell structure, and operating conditions [33]. For example, a reduced CO tolerance was found due to ruthenium dissolution from the anode catalyst particles caused by cell reversal during

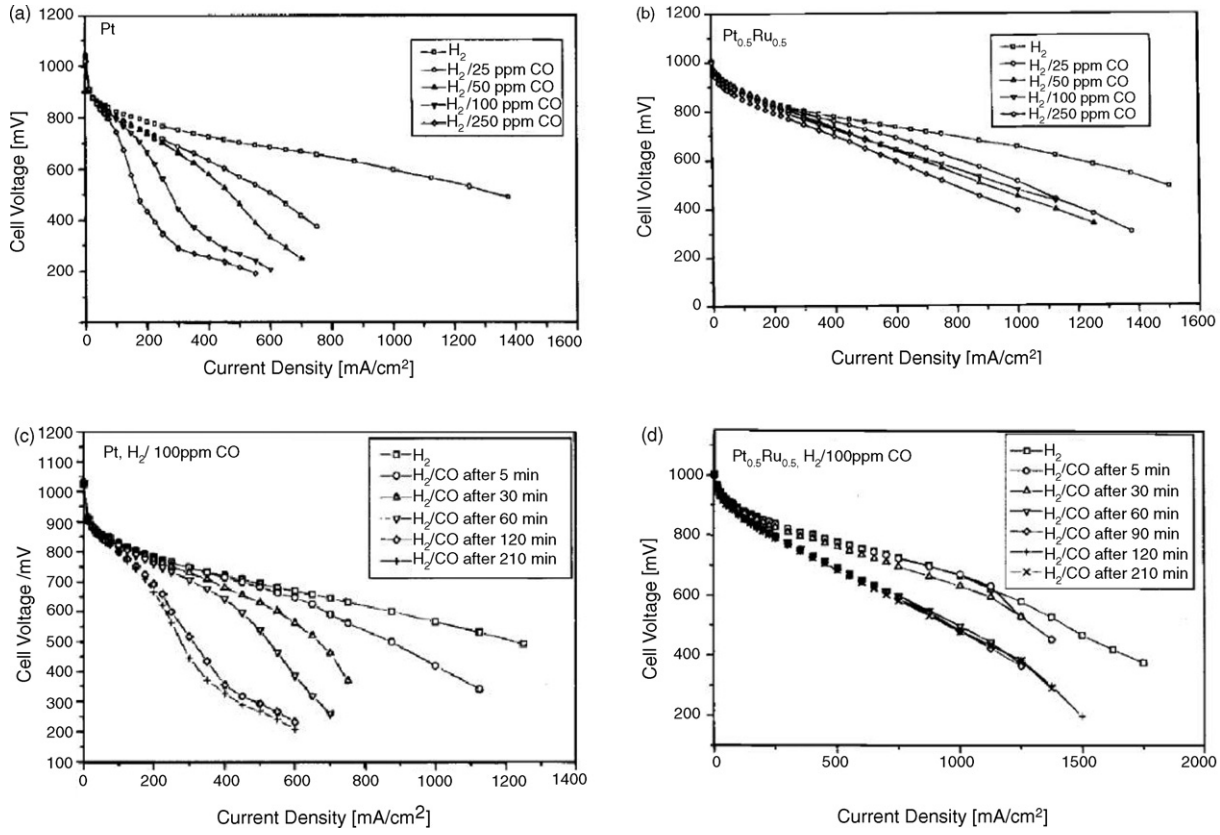

Fig. 6. Effects of CO concentration and exposure time on cell performance for different anode catalysts [31]. $A = 4\,cm^2$; cathode catalyst: pure Pt; catalyst loadings: $1\,mg\,cm^{-2}$; Nafion® 117; $T_{cell} = 80\,^{\circ}C$. (a) and (c) Pt; (b) and (d) $Pt_{0.5}Ru_{0.5}$.

PEM fuel cell operation with fuel starvation [34]. Significant work has been done in an effort to improve both catalyst CO tolerance and cost-effectiveness. To address this, a brief review of recent developments in CO tolerance anode electrocatalysts will be provided in a later section on mitigation.

3.1.1.4. Other CO effects. Hydrogen dilution effects by other inert gases such as nitrogen [35] were also examined, and lower performance compared to that with a pure hydrogen feed was observed. Even a trace amount of CO as low as 10 ppm in the diluted hydrogen could cause a significant performance drop [36]. The performance loss became even deeper with more diluted hydrogen [36,37]. This was rationalized by the amplification effect of hydrogen dilution on CO poisoning.

The presence of CO impurities in the anode hydrogen fuel could also significantly affect the cathode performance as a result of CO crossover from anode to cathode, probably primarily through pin-holes in the membrane [38,39].

The increases in anode hydrogen flow rate and cathode oxygen pressure [40], as well as in low catalyst loading [41], were all found to substantially facilitate the CO poisoning.

3.1.1.5. Evaluation and detection of CO poisoning. Developing analytical methods or diagnostic tools for the evaluation of CO contamination in a fuel cell environment is both important and necessary. An experimental method using a polymer membrane combined with a gold wire was suggested for performing a quantitative evaluation [42]. The results revealed that hydrogen containing as low as 10 ppm CO or air did not significantly affect the anode performance. However, 100 ppm CO poisoned the anode catalyst, resulting in a remarkable increase of anodic overpotential [42]. A technique using a "first order plus dead time" model was employed to diagnose CO transients in PEM fuel cells [43]. An analytical method involving poisoning prediction formulas and estimation coefficients has been proposed to quantitatively compare the extent of CO poisoning in Pt and PtRu anode catalysts with fuels containing different CO concentrations under fixed operating conditions [44]. Sensors that can detect CO concentrations as low as 50 ppm in H_2-rich gas streams at 68 °C [45] or as low as 10 ppm in reformate streams at room temperature [46] have also been developed.

Electrochemical and surface analytical methods are commonly used to detect CO adsorption on the Pt electrodes. Cyclic voltammetry, including CO-stripping voltammetry combined with either X-ray photoelectron spectroscopy [47] or scanning electrochemical microscopy, [48] was shown to be useful in a study of CO adsorption/oxidation. Electrochemical impedance spectroscopy (EIS) is another powerful method to characterize various electrochemical processes involved in a PEM fuel cell. EIS has been used for kinetic analysis of CO poisoning [28,49–54], and evaluation of CO-tolerance with different anode catalysts at various temperatures [50,52,55]. A combination among *in situ* stripping voltammetry, current–voltage polarization, and EIS methods were used to perform a quan-

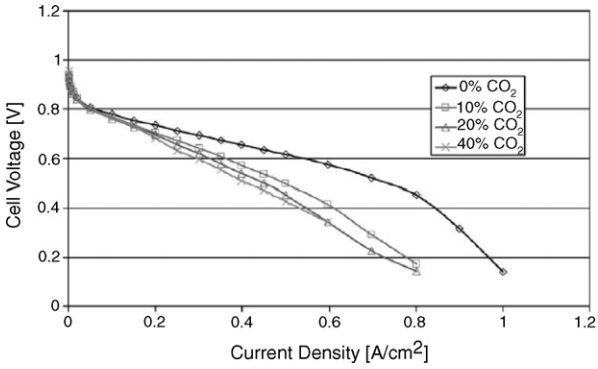

Fig. 7. Effect of CO_2 concentration on cell performance [57]. Anode = cathode = 0.35 mgPt cm^{-2}, E-TEK ELAT gas diffusion electrode, Nafion 105, T_{cell} = 60 °C, P = 1.5 bar.

titative analysis of H_2-oxidation polarization loss induced by CO poisoning on Pt-based gas diffusion electrodes [51]. However, extra care must be taken when using EIS techniques, as pointed out in a recently published paper [56], due to a possible misinterpretation of CO poisoning effects, when there is a possibility of interference due to fuel cell flooding.

3.1.2. *Influence of carbon dioxide*

Currently, approximately 95% of hydrogen is produced by steam reforming of natural gas (CH_4), which produces a high level of carbon dioxide (25% [57]) as a by-product. As shown in Fig. 7, the performance loss due to CO_2 contamination in anode fuel can be observed especially at higher current densities [57]. A performance loss of 30% occurred at 0.5 V with a 20% CO_2 content [58]. On a Pt catalyst, CO_2 can be catalytically converted into CO, which then poisons the catalyst. Thermodynamic calculations [58] revealed that approximately 20–100 ppm CO in equilibrium concentrations can be produced by a water-CO_2 gas shift reaction (WGSR):

$$2Pt + H_2 \rightarrow 2Pt\text{–}H_{ads} \quad (1)$$

$$CO_2 + 2Pt\text{–}H_{ads} \rightarrow Pt\text{–}CO_{ads} + H_2O + Pt \quad (2)$$

The CO concentration can be increased with decreased temperature and water content in the anode feed [58].

A kinetic model assuming the formation of adsorbed CO species on a Pt/C catalyst by a WGSR mechanism was proposed to describe cell performance deterioration in the presence of small amounts of CO_2 [59]. This model was validated by the observed CO coverage measured through CO-stripping experiments [35]. Even at a low CO_2 level of 1%, enough CO could be produced through the WGSR mechanism to poison more than 50% of surface Pt sites, resulting in a significant increase in anodic overpotential [60]. The CO_2 poisoning effects were sensitive to the nature of the catalyst materials and could be enlarged by increasing the reaction rates of WGSR [58]. It was also found that a stable adlayer consisting mainly of linear-, bridge- and multi-bonded CO on the Pt surface could effectively suppress the reaction between CO_2 and pre-adsorbed hydrogen, especially at low temperatures with the PtRu/C catalyst [61].

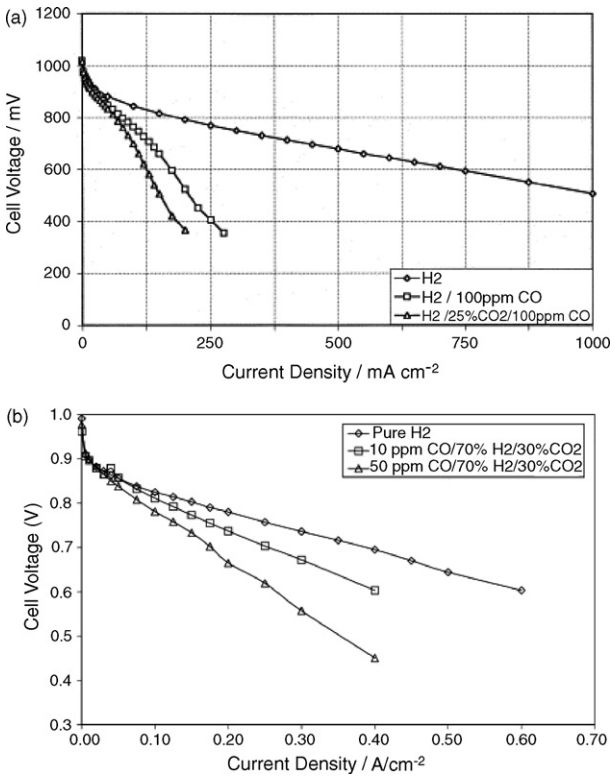

Fig. 8. Effect of CO and CO_2 on cell performance [27,39]. (a) A = 10 cm^2, Pt and PtRu = 1 mg cm^{-2}, Nafion 117 membrane, T_{cell} = 80 °C [27]; (b) A = 10 cm^2, Pt = 1.7 mg cm^{-2}, PtRu = 0.60 mg cm^{-2}, Nafion 1135 membrane, T_{cell} = 70 °C [39].

A synergetic poisoning effect of CO and CO_2 was investigated by adding 25% CO_2 to a H_2/CO (100 ppm) stream. The enlarged catalyst poisoning effect was observed with a Pt/C catalyzed electrode at a cell temperature of 80 °C [27]. However, a recent study found that the influence of CO_2 reduction was insignificant if the fuel streams contained a trace impurity of CO. The presence of CO could lead to a higher coverage of CO on the Pt surface, which then suppressed the reduction of CO_2 to CO [62]. However, the majority of the work recognized that the presence of both CO and CO_2 in fuels might have an accumulated influence on cell performance. For example, as shown in Fig. 8(a), compared with pure hydrogen, 100 ppm CO in the fuel can significantly degrade the cell performance. When 25% CO_2 is added in this 100 ppm CO-containing fuel, a further performance drop can be observed [27]. As seen in Fig. 8(b), in the presence of 30% CO_2, even a small level of CO (30–50 ppm) can cause a remarkable decrease in cell performance, particularly at higher current densities [39].

3.2. *Influence of hydrogen sulphide*

Hydrogen sulphide (H_2S), an even more severe fuel contaminant than CO, has been investigated extensively [9,30,63–65]. A trace amount of H_2S, when exposed to an anode or cathode, was found to degrade the cell performance significantly, mainly through the poisoning effect of the Pt catalysts [63]. As shown in Fig. 9, Knights et al. [9] found that at 100 mA cm^{-2}, 80 °C,

Table 2
Model equations in the presence of various contaminants [9]

Contaminant	Equation	
CO, H_2S in fuel	$E_c = E_0 - (b_1 + K_{cK}C) \times \log i - R_0 i + K_{cK}C \times \log i \times \left(\frac{1}{1 + K_1 \exp(K_2 t)}\right)$	(3a)
NO_2, SO_2 in air	$E_c = E_0 - (b_1 + K_{cK}C) \times \log i - R_0 i + K_{cK}C \times \log i \times \exp(-K_3 t)$	(3b)
NH_3 in air and fuel	$E_c = E_0 - b_1 \times \log i - (R_0 + K_{CR}C)\, i + K_{CR}Ci \exp(-K_4 t)$	(3c)

1.2 ppm H_2S could cause a cell voltage drop greater than 300 mV within 25 h. The voltage loss behaviour could be described by the combined theoretical and empirical model based on fuel cell polarization theory [66–68] given in Table 2 [9]. As is evident in Fig. 9, the experimental data fit reasonably well with the model-simulated lines.

In Eq. (3), E and i are potential and current density, respectively. E_0 is given by [69]

$$E_0 = E_r + b \log i_0 \quad (4)$$

where E_r is the reversible potential for the cell, i_0 and b are the Tafel parameters for oxygen reduction, and R_0 is the ohmic resistance. K_{cK}, K_{CR}, K_1, K_2, K_3, and K_4 in Eqs. (3a)–(3c) are constants which account for contamination, C is the concentration of contaminant, and t is the contamination time.

A 0.1 ppm level of H_2S in the fuel stream could cause a 250 mV cell voltage drop within 300 h at 0.5 A cm^{-2} load [9]. This poisoning effect was also sensitive to the cell operation temperatures and load level [9,65]. Large performance losses were measured at H_2S concentrations as low as 50 ppm at 70 °C when the fuel cell anode was exposed to the H_2S-containing fuel for 3.8 h. Unlike the case of CO poisoning, the presence of Ru in the Pt catalyst could not provide sufficient tolerance to H_2S poisoning [30].

3.3. Influence of ammonia

The extent of performance deterioration due to the presence of ammonia depends on the concentration level and exposure time [57,70–72]. As shown in Fig. 10, high NH_3 concentration resulted in a large cell voltage loss (Fig. 10(a)) and a 15-h exposure to 30 ppm NH_3 in the anode fuel caused a rapid drop in cell performance (Fig. 10(b)) [70]. The performance loss could be partially recovered after 17 h, but no further improvement was achieved beyond this time. It was believed that NH_3 contamination reduces the proton conductivities of both the Nafion membrane and the anode catalyst ionomer layer [70,73]. On the other hand, NH_3 crossover from anode to cathode could also contaminate the cathode of a fuel cell [73].

3.4. Influence of cationic ions

The foreign cationic ions that originate from impurities in fuel cell stack component materials, fuels, and coolants can cause water management problems in fuel cells. The cationic ions such as alkali metals, alkaline earth metals, transition metals, and rare earth metals were reported to directly affect the transport properties of the electrolyte membrane [74–82]. Iron ions from stainless steel end plates resulted in severe Nafion degradation as evidenced by a massive fluoride loss [83]. The iron contami-

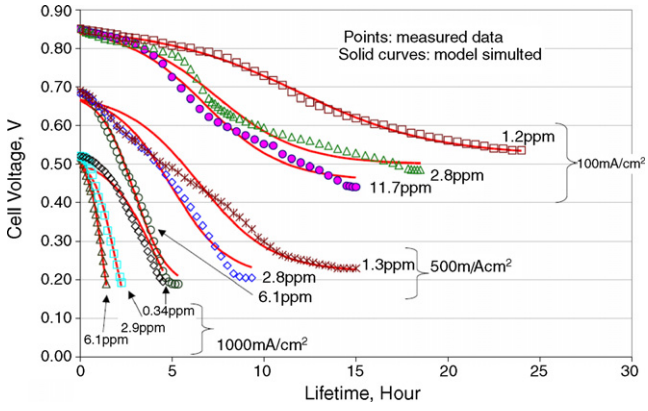

Fig. 9. Effect of H_2S contamination on cell performance and lifetime. Pt loading at 1.0 mg cm^{-2}, Nafion 112, and 80 °C [9].

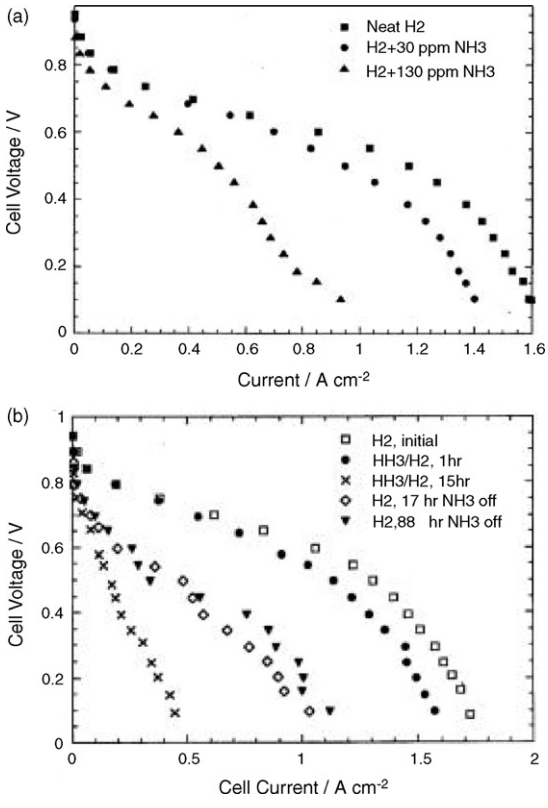

Fig. 10. Effects of ammonia concentration and exposure time on cell performance at 80 °C [70]. (a) Different concentrations; (b) long-term exposure to 30 ppm NH_3 in the anode feed stream.

nation also led to several types of performance losses, including cathode and anode kinetic losses, ohmic loss, and mass transport loss [7]. For example, metallic ions including Cu^{2+}, Fe^{3+}, Ni^{2+}, and Na^{+} presented in sulphate salt solutions at a concentration level of 100 ppm were found to significantly decrease the ionic conductivity of a Nafion 117 membrane; among these the ferric ions were more harmful [75,84]. Collier et al. [20] discussed the critical role played by trace metallic ions in membrane degradation by reviewing the degradation modes of polymer electrolyte membranes. They concluded that the displacement of H^{+} with foreign cationic ions directly affected water flux and proton conductivity inside the membrane, leading to membrane degradation.

3.5. Influence of air pollutants

Air pollutants listed in Table 1 can cause various contamination problems during fuel cell operation. For example, a "morning voltage drop" in a fuel cell stack was observed when performance tests used compressed air as a cathode feed stream. This morning drop has been identified as being caused by air pollutants such as NO_x and SO_x [9]. In the literature, several air pollutants such as NO_x, SO_x, H_2S [6,9,16], and NH_3 [9] have been investigated with respect to their contamination effects. When air contains acidic pollutants such as SO_x (SO_2 and SO_3), the MEA pH is depressed, resulting in free acid in the cell and causing potential problems. In the presence of SO_2 in the air stream, the fuel cell current density dropped by over 50% [17]. A complete deterioration of cell performance occurred with cathode exposure to 200 ppm H_2S for 10.5 h [16]. Knights et al. [9] reported that SO_2 and H_2S adversely influenced fuel cell performance. A combined contamination effect was found when the cathode was fed $NO_2 + SO_2$ and the anode was fed H_2S, as shown in Fig. 11 [9], which appears to be simply additive results of each contaminant. However, the performance loss induced by the presence of NO_2 could be recovered by reintroducing neat air into the contaminated cathode [17]. For SO_x and H_2S contamination, the performance losses seemed to be partially recoverable [9,17].

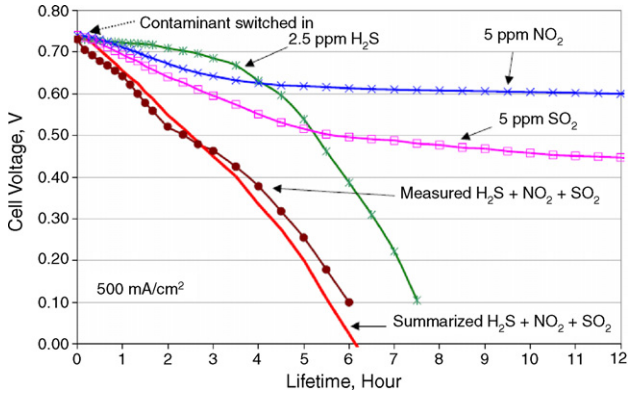

Fig. 11. Individual and combined effects of 5 ppm NO_2 and 5 ppm SO_2 in air and 2.5 ppm H_2S in fuel on cell voltages and lifetime [9]. Symbols represent experimental data, while solid lines show model simulation. Total Pt loadings at 1.0 mg cm^{-2}, Nafion 112 and 500 mA cm^{-2}.

A comparison between the cyclic voltammograms obtained with a clean MEA and with a NO_2-contaminated MEA revealed that the NO_2 poisoning did not involve catalyst surface poisoning species; only the ionomer and/or the catalyst–ionomer interface were affected [17]. It was speculated that the poisoning species might be NH_4^{+} formed through the electrochemical reduction of NO_2 at the cathode,

$$NO_2 + 8H^{+} + 7e^{-} \rightarrow NH_4^{+} + 2H_2O \quad (5)$$

which could compete with the O_2 reduction reaction for catalyst active sites [17]. Surface cyclic voltammetry was also used to identify the surface adsorption of NO on a cathode Pt catalyst surface [10]. A linear relationship between surface coverage and NO concentration was observed. The performance degradation with NO_x present in the air stream was also observed by a recent electrochemical impedance measurement [16]. In battlefield environments, the fuel cells used as portable power sources could severely suffer from contamination induced by sulfur dioxide, carbon monoxide, propane, and benzene, as well as by chemical warfare agents [15]. Ammonia could also affect the cathode performance, but much less severely than NO_x, SO_x, and H_2S [9].

3.6. Effect of other impurities

Nafion membrane contamination caused by silicon dissolved from the sealing gaskets and by impurities in the coolant were reported to be the main causes for the rapid decline in fuel cell performance after continuous operation for 18:00 h [18]. In addition, high concentrations of nitrogen in the anode fuel could also cause performance drop, especially at higher current densities [35]. This N_2 effect can be attributed mainly to dilution. The effects on fuel cell performance of hydrogen and oxygen diluted by N_2 were also characterized by impedance spectra. Three loops were associated with hydrogen oxidation, oxygen reduction, and a low-frequency diffusion process which is likely linked to the diffusion of oxygen in nitrogen [85].

4. Poisoning mechanisms

4.1. Fundamental understanding

The contamination effects of trace impurities on fuel cell performance have been substantially investigated and reported as phenomenon observations. The corresponding contamination mechanisms are not well understood, mainly due the lower priority of contamination in fuel cell R&D, and also partially due to the complexity of the contamination processes. Among those impurities being investigated, CO contamination is the most extensively studied and best documented, due to its relative simplicity with respect to surface poisoning and oxidation. Even so, the CO poisoning mechanism remains controversial and needs to be further clarified. This section provides a general overview for the fundamental understanding of the poisoning mechanisms of typical contaminants, namely carbon oxides, sulfur-containing species, ammonia, and cationic ions, followed by a brief summary of model studies from the literature.

4.1.1. Carbon monoxide

Platinum has been recognized as the best electrocatalyst for hydrogen and oxygen reactions. Unfortunately, Pt can be easily poisoned in the presence of carbon oxides. It is well known that CO poisons hydrogen electro-oxidation on the Pt surface, particularly at the operational temperatures of PEM fuel cells. The strong adsorption of CO at the Pt electrode can directly block the surface active sites used for H_2 electro-oxidation. The representative mechanism can be expressed as follows [86]:

(1) Dissociative chemisorption

$$H_2 + 2Pt \rightarrow 2Pt\text{–}H_{ads} \quad (6)$$

$$CO + Pt \rightarrow Pt\text{–}CO_{ads} \quad (7)$$

$$2CO + 2Pt\text{–}H_{ads} \rightarrow 2Pt\text{–}CO_{ads} + H_2 \quad (8)$$

(2) Electro-oxidation reaction

$$2Pt\text{–}H_{ads} \rightarrow 2Pt + 2H^+ + 2e^- \quad (9)$$

Reaction (6) requires two adjacent bare Pt sites and therefore is quite slow. Reaction (9) is relatively fast. The adsorption of CO occurs not only at bare Pt sites through Reaction (7) but also at Pt hydride sites via Reaction (8). It is believed that a linear-absorbed CO species involves one adsorption site per CO molecule, while a bridge-bonded CO species requires two adjacent Pt surface sites [87,88]. The linear- and bridge-bonded CO absorptions can be schematically illustrated as shown below:

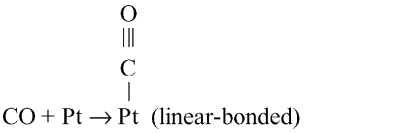

(7a)

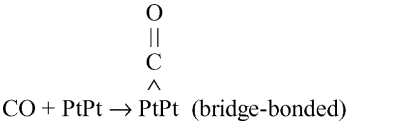

(7b)

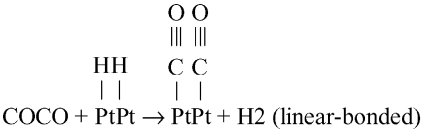

(8a)

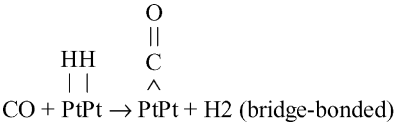

(8b)

Thus, one bridge-bonded CO molecule can block more than one H site and linear-bonded CO adsorption requires only one site. Therefore, linear-bonded CO should have higher CO coverage. Direct experimental evidence for Pt-site poisoning by adsorbed CO is provided in Fig. 12, which shows the effect of CO coverage on kinetic currents (I_k) of hydrogen oxidation on a Pt surface at ambient temperature [88]. A linear decrease in I_k with increasing CO coverage was observed. In addition, the CO coverage was found to depend upon the electrode surface state (surface roughness) and the atmosphere of the electrode/electrolyte interface (partial pressure of CO) [88].

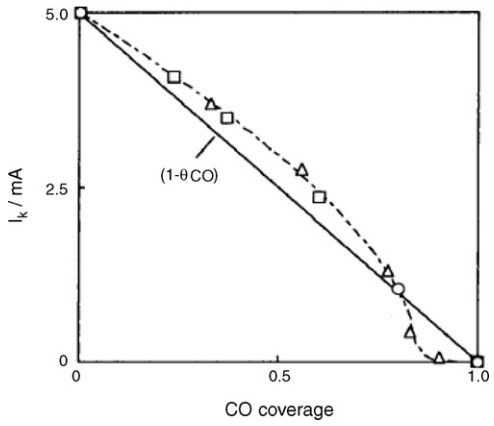

Fig. 12. Kinetic currents for H_2 oxidation on Pt surface at 20 mV (vs. RHE) and 26 °C as a function of CO coverage [88].

The elimination of adsorbed CO can be described by the following reactions:

$$Pt + H_2O \rightarrow Pt\text{–}OH_{ads} + H^+ + e^- \quad (10)$$

$$Pt\text{–}CO_{ads} + Pt\text{–}OH_{ads} \rightarrow 2Pt + CO_2 + H^+ + e^- \quad (11)$$

The poisoned Pt sites are ineffective for CO electrocatalytic oxidation since water cannot be readily adsorbed at Pt sites to produce oxygen-containing species via Reaction (10) at an electrode potential of 0.5 V versus NHE. Reaction (11) takes place at even higher electrode potentials (~0.6 V versus NHE). At potentials below the oxide formation (Reactions (10) and (11)), a near-zero rate constant for hydrogen electro-oxidation was obtained using scanning electrochemical microscopy on a CO-covered polycrystalline Pt in sulfuric acid solutions. However, on a CO-free Pt electrode, the obtained rate constant was larger than 1 cm s^{-1} [48]. This clearly demonstrates that CO adsorption can significantly reduce the H_2-oxidation rate, resulting in a fuel cell performance drop. On the other hand, the H_2-oxidation rate in the presence of CO is also dependent on several other factors including electrode structure, operating conditions, electrolytes, and, most importantly, electrocatalysts.

A popular method for improving the oxidation rate of H_2 in the presence of CO is to use CO-tolerant electrocatalysts. Pt alloying with a second metal (binary) or more than one metal (ternary or quaternary) can form catalysts that are more CO tolerant than the pure Pt catalyst. Two models were proposed to interpret a change of CO sensitivity to H_2 oxidation induced by Pt alloying. One is a bifunctional model involving a promotion mechanism, and the other is an electronic model dealing with an intrinsic mechanism. The bifunctional mechanism suggests that water activation is first initiated by the second alloying metal (M_e) to form M_e–OH_{ads}, which then reacts with a neighbouring CO-adsorbed Pt atom to complete CO oxidation:

$$M_e + H_2O \rightarrow M_e\text{–}OH_{ads} + H^+ + e^- \quad (12)$$

$$Pt\text{–}CO_{ads} + M_e\text{–}OH_{ads} \rightarrow Pt + M_e + CO_2 + H^+ + e^- \quad (13)$$

This mechanism was supported by experimental data obtained using PtRu as a catalyst by CO stripping [89] and rotating disc electrode [90,91] methods. Limitations of this mechanism have

been discussed in several PtRu catalyst-related investigations [87,92].

The intrinsic mechanism indicates that the alloying effect can decrease the stability of CO bonding more than that of H on the catalyst surface through modifying the electronic properties of the pure noble metal by another metal. This mechanism was confirmed by experimental studies on PtRu catalyst electrodes [93,94] and Pt-WO_3 electrocatalysts [95]. Theoretical analyses based on density functional calculations and Monte Carlo simulations for $Pt_{0.5}Ru_{0.5}$ alloy catalyst were also consistent with this mechanism [96].

If a fuel cell can bear a higher concentration contaminant such as CO, one says that this fuel cell has high CO tolerance. A fuel cell catalyzed by a Pt-alloy catalyst obviously has higher CO tolerance, and the catalyst, such as $Pt_{0.5}Ru_{0.5}$, is called a CO-tolerance catalyst. In the literature, the fuel cell contamination tolerance is defined as the presented maximum contaminant concentration (in ppm) at which the fuel cell can still give a desired cell voltage at desired current density. The CO tolerance values were reported from a few (2 to 5) ppm up to 10,000 ppm, depending on several factors including electrode structure, operating conditions, electrolytes, and electrocatalysts, of which electrocatalysts are a major factor. Contamination tolerance catalysts will be further discussed in the section on mitigation methods, below.

4.1.2. Carbon dioxide

As discussed for Reaction (2), $Pt–CO_{ads}$ can be formed in the presence of CO_2 through a WGSR mechanism, which is similar in chemical formula to that formed by CO direct adsorption. The formed adsorption species on the Pt surface from either Reactions (7) and (8) or Reaction (2) can be electro-oxidized at higher electrode potentials ($\geq$0.7 V versus NHE) via the "reactant pair mechanism" [97]:

$$Pt–CO_{ads} + Pt–O_{ads} \rightarrow CO_2 + 2Pt \quad (14a)$$

$$Pt–CO_{ads} + Pt–OH_{ads} \rightarrow CO_2 + H^+ + e^- + 2Pt \quad (14b)$$

However, the exact structure and adsorption form of surface species formed by CO_2 reduction have not yet been clarified. It could have linear-, bridge- or triple-bonded CO structure [98–103]. The CO/COOH radicals [104], $COOH_{ads}$ and COH_{ads} [103,105–108], have also been reported.

4.1.3. Hydrogen sulphide and sulfur dioxide

Sulfur-containing species such as sulfur dioxide and sulfur hydrogen are usually present as impurities in the fuel and air streams of a fuel cell. Even small amounts of S impurities can cause significant performance drop. Similar to CO adsorption, H_2S and SO_2 also strongly adsorb on the Pt catalyst. The adsorption of S-containing species to the active sites of a catalyst, occupying the polyatomic sites, prevented the reactants, including oxygen and hydrogen, from adsorbing at the catalyst surface. A platinum electrode surface in an aqueous solution containing H_2S reacted with H_2S to form $Pt–S_{ads}$ and H_2 [109]:

$$Pt + H_2S \rightarrow Pt–S_{ads} + H_2 \quad (15)$$

or to form platinum hydrogen sulphide and platinum hydrogen through the following paths [110]:

$$Pt + H_2S \rightarrow Pt–H_2S_{ads} \quad (16a)$$

$$Pt + HS^- + H^+ \rightarrow Pt–HS_{ads}{}^- + H^+ \quad (16b)$$

$$Pt–HS_{ads}{}^- + H^+ \rightarrow Pt + H_2S \quad (17)$$

$$Pt + H^+ \rightarrow Pt^+–H_{ads} \quad (18)$$

where Pt^+ represents an equivalent positive charge on the Pt surface. The following reaction is also possible due to an electrochemical potential resulting from Reactions (17) and (18) [110]:

$$2Pt + H_2S \rightarrow Pt–SH_{ads} + Pt–H_{ads} \quad (19)$$

Further oxidation of the adsorbed SH and H_2S formed platinum sulphide [110]:

$$Pt–SH_n \rightarrow Pt–S_{ads} + nH^+ + ne^- \ (n = 1 \text{or} 2) \quad (20)$$

The results from the first-principle calculation confirmed that the adsorbed H_2S and SH are highly unstable on Pt(1 1 1), while the adsorbed S and H are the most stable SH_n (n = 0, 1, 2) intermediates on Pt(1 1 1) [111]. The formation of $Pt–S_{ads}$ on the catalyst surface makes it impossible for the fuel cell to recover from contamination [9].

With respect to SO_2, Contractor and Lal [112] reported that the end products of SO_2 adsorption on a Pt electrode would be linearly and bridged adsorbed S species. These two forms of chemisorbed S species on Pt at 80 °C were reported to be responsible for catalyst poisoning [113]. Electrochemical reduction from SO_2 to S on a Pt electrode, producing SO intermediates, was also suggested [114]:

$$Pt + SO_2 + 2H^+ + 2e^- \rightarrow Pt–SO_{ads} + H_2O \quad (21)$$

$$Pt–SO_{ads} + 2H^+ + 2e^- \rightarrow Pt–S_{ads} + H_2O \quad (22)$$

The formation of the SO species could also lead to difficulties in oxygen reduction.

4.1.4. Ammonia

It was suggested that NH_3 might not easily adsorb on the carbon fibres in the gas diffusion layer. However, it would react with protons in the membrane, thus staying in the membrane phase and decreasing the membrane conductivity by forming $NH_4{}^+$ [70,71]:

$$NH_3\,(g) \rightarrow NH_3\,(\text{membrane}) \quad (23)$$

$$NH_3\,(\text{membrane}) + H^+ \rightarrow NH_4{}^+ \quad (24)$$

The strong acid in perfluorosulfonic acid ionomers can stabilize an ammonium ion in the membrane phase, resulting in Reaction (24) being shifted to the right. As shown in Fig. 13, there is a linear decrease in membrane conductivity induced by the ammonium species in a Nafion 117 membrane phase [73]. Reaction (24) could also take place with the ionomer inside the catalyst layers. On the other hand, the ammonium species formed at the anode catalyst layer, when presented as an anode fuel impurity,

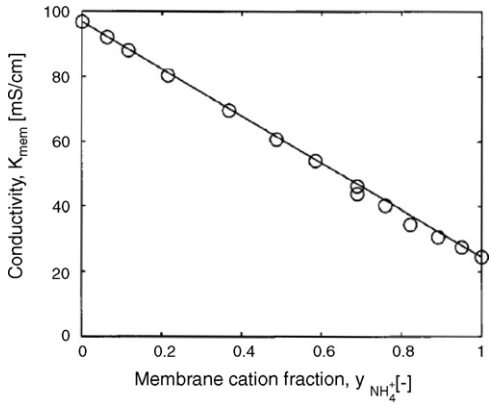

Fig. 13. Dependence of membrane conductivity in membrane cation fraction at 25 ± 0.1 °C for Nafion® 117 [73].

could be further transported to the cathode catalyst layer through the membrane, degrading the performance of both the anode and the cathode.

4.1.5. Cationic ions

The most detrimental effect of trace cationic ions is the contamination of membranes. Many cationic species exhibit a high affinity for the sulfonic groups in Nafion membranes. Previous results obtained by streaming potential measurement for Nafion® 117 indicated that a cation with a higher charge density and higher hydration enthalpy tended to carry more water molecules during transport [82]. The diffusion and transport characteristics of protons and water were found to be directly affected by the exchange between cationic ions and protons [74,77,80–82]. A cluster network model indicated that for a given hydration state, the membrane resistance followed an inverted sequence with respect to the radius of the dehydrated cation [79]. As a result, a lower proton ionic conductivity was observed, which increased the fuel cell membrane polarization. This cation exchange with the proton inside the membrane can also result in membrane dehydration and water management problems [76].

A simplified model developed by Okada et al. [115] predicted that a cationic impurity presented at an interface of the anode and membrane would result in a serious membrane dehydration problem. In addition, the presence of minor impurities of Fe^{2+} and Cu^{2+} can accelerate the decomposition of the electrolyte membrane, due to the formation of oxygen radicals caused by the reaction with hydrogen peroxide according to Reactions (25)–(29) [78]:

$$H_2O_2 + Fe^{2+} \rightarrow HO^{\bullet} + OH^- + Fe^{3+} \quad (25)$$

$$Fe^{2+} + HO^{\bullet} \rightarrow Fe^{3+} + OH^- \quad (26)$$

$$H_2O_2 + HO^{\bullet} \rightarrow HO_2^{\bullet} + H_2O \quad (27)$$

$$Fe^{2+} + HO_2^{\bullet} \rightarrow Fe^{3+} + HO_2^- \quad (28)$$

$$Fe^{3+} + HO_2^{\bullet} \rightarrow Fe^{2+} + H^+ + O_2 \quad (29)$$

This mechanism could lead to membrane thinning or the formation of a pin-hole. Collier et al. [20] provided a comprehensive review of membrane degradation due to cationic ion contamination.

4.2. Model studies

Theoretical models are important tools for the fundamental understanding of contamination mechanisms, degradation prediction, and the development of mitigation technology. Most reported modeling studies have concentrated on CO contamination [37,116–122]. Earlier studies of anode CO poisoning were reviewed by Baschuk and Li [21]; readers are referred to that review for further information. Springer et al. [37,117] developed a steady-state theoretical anode model for PEM fuel cell operation on reformate feed. They considered the kinetics of the following reactions:

$$CO + M \underset{b_{fc}(\theta_{CO})k_{fc}}{\overset{k_{fc}}{\longleftrightarrow}} (M\text{–}CO) \quad (30)$$

$$H_2 + 2M \underset{b_{fh}k_{fh}(\theta_{CO})}{\overset{k_{fh}(\theta_{CO})}{\longleftrightarrow}} 2(M\text{–}H) \quad (31)$$

$$(M\text{–}H) \xrightarrow{k_{eh}} H^+ + e^- + M \quad (32)$$

$$H_2O + (M\text{–}CO) \xrightarrow{k_{ec}} M + CO_2 + 2H^+ + 2e^- \quad (33)$$

where M represents a catalyst site. The steady-state surface coverage can be calculated according to the kinetics of adsorption, desorption, and charge-transfer fluxes of CO and H_2, as in Eqs. (34) and (35).

$$\rho\frac{d\theta_{CO}}{dt} = k_{fc}\chi_{CO}P_A(1-\theta_{CO}-\theta_H) - b_{fc}k_{fc}\theta_{CO} - k_{ec}\theta_{CO}e^{((V_a+V_{Nernst})/b_c)} = 0 \quad (34)$$

$$\rho\frac{d\theta_H}{dt} = k_{fh}\chi_h P_A(1-\theta_{CO}-\theta_H)^n - b_{fh}k_{fh}\theta_H^n - 2\theta_H k_{eh}\theta_{CO}\sinh\left(\frac{V_a+V_{Nernst}}{b_h}\right) = 0 \quad (35)$$

where θ_{CO}, θ_H are fractional surface coverage of CO and hydrogen, respectively; ρ is molar area density of catalyst sites mol cm^{-2}; χ_i is molar fraction of species i; P_A is total pressure, atm; V_a is local anode potential in the catalyst layer, V; V_{Nernst} is Nernst potential $RT\ln(P_A\chi_h)$, V. Eq. (36) gives current density expressions for hydrogen and CO oxidation.

$$j_h = 2k_{eh}\theta_H\sinh\left[\frac{V_a+V_{Nernst}}{b_h}\right],$$
$$j_{CO} = 2k_{ec}\theta_{CO}e^{((V_a+V_{Nernst})/b_c)} \quad (36)$$

Analytic solutions for θ_H and θ_{CO} were obtained assuming the rate constants are independent of θ_{CO} (Langmuir isotherm). In the actual calculation of surface coverage, both Langmuir and Temkin isotherms were employed, even though the equations were derived from a Langmuir isotherm. The model incorporates diffusion losses in the anode gas diffusion layer and diffusion and ohmic losses in the anode catalyst layer. It defines the distribution of the hydrogen reactant as a function of the location

along the catalyst layer adjacent to the backing at a given composition in the flow channel. Having defined local hydrogen and CO concentrations, the model provides detailed equations for interfacial kinetics that apply for hydrogen electro-oxidation at Pt in the presence of CO. The study illustrated that a Temkin isotherm can provide better agreement with experimental data in terms of steady-state cell performance. With this model, the paper further explored effects of varying kinetic parameters on cell performance. The study showed that, whereas fuel dilution and high utilization do not penalize cell performance in the absence of CO, the voltage loss under similar conditions can be large when CO is present. This is attributed to there being no "correctable" local low-hydrogen mole fraction in the presence of CO. Replacement of Pt by PtRu is likely to enable operation with 10 ppm CO in neat hydrogen, and possibly in reformate at low fuel utilization. However, with diluted anode feed streams and under high fuel utilization, such an anode catalyst is less likely to resolve the tolerance problem even at 10 ppm CO.

Baschuk et al. [120,121] formulated a steady-state CO poisoning model which applied the conservation principle to the electrode backing, catalyst layers, and polymer electrolyte. Specifically, conservation of species and thermal energy were applied along with the Stefan–Maxwell equation for multi-component gas diffusion and Fourier's Law for heat conduction. Darce's Law was used for the full momentum equation. Electron migration in the solid phase of the electrode backing and catalyst layer was modeled with Ohm's Law. The flux of protons and water was described by the Nernst–Planck equation. Oxygen reduction at the cathode was modeled using the Butler–Volmer equation, while the adsorption, desorption, and electro-oxidation of hydrogen and CO at the anode were modeled by the Tafel–Volmer and "reactant pair" mechanism, respectively. Temkin kinetics was applied for CO adsorption and desorption and the Langmuir model was assumed for hydrogen adsorption and desorption. This study demonstrated that the Temkin model provides superior agreement with experimental data and the Langmuir model cannot be used as a model for CO adsorption and desorption in a PEM fuel cell. The model predictions of cell polarization with contaminant levels of 0–100 ppm were compared with experimental data. Excellent agreement between the model and experimental data were observed. The study also illustrated that increasing the operating pressure increases the performance of the PEM fuel cell at low current densities, but decreases the performance at high current densities due to membrane dehydration.

Bhatia and Wang [119] studied the transient behaviour of CO contamination with diluted hydrogen fuel based on Springer's kinetic model. In their model, the surface reaction kinetic parameters were assumed to be constant (Langmuir model) while surface coverage, current density and cell voltage equations were solved numerically. The model simulations were compared with experimental data. The results showed that at high contaminant levels (100 ppm CO, 100% H_2 and 100 ppm CO, 40% H_2), the model can reproduce the experimental data. At low contaminant levels (10 ppm CO, 100% H_2 and 10 ppm CO, 40% H_2), the fit is poor. Their results demonstrated that, while hydrogen dilution alone lowers the fractional coverage on the catalyst surface, it is only when CO is present that the coverage is lowered to a degree that affects cell voltage. Under this condition, the addition of hydrogen dilution will compound the low surface coverage problem even further, and thus cause very poor cell performance. Even with low CO levels normally considered safe for cell operation (10 ppm), hydrogen dilution can cause an extremely severe loss of cell polarization.

The effect of CO crossover to the cathode was studied by Rama et al. [118]. They formulated a 1D steady-state, low-temperature, isothermal, isobaric PEMFC model with multi-species input. The simulation results indicated that the CO concentration at the cathode–membrane interface does not vary significantly with respect to current density. This is due to the fact that the CO flux in the anode and membrane is at least two orders of magnitude smaller than the H_2 flux at a current density of 0.1 A cm^{-2} and up to three orders of magnitude smaller at higher current densities. The simulated cathode polarizations with fuel CO contamination agreed well with published experimental data.

CO_2 anode contamination modeling was reported by Janssen [59]. In this model WGSR (Reaction (2)) is assumed to be the origin of the CO_2 poisoning effects. The following reactions were considered in the kinetic model:

$$H_2 + 2M \underset{k_d}{\overset{k_a}{\longleftrightarrow}} 2(M\text{–}H) \tag{37}$$

$$2(M\text{–}H) \xrightarrow{k_{eh}} 2H^+ + 2e^- + 2M \tag{38}$$

$$CO + M \underset{k_{dc}}{\overset{k_{ac}}{\longleftrightarrow}} (M\text{–}CO) \tag{39}$$

$$H_2O + (M\text{–}CO) \xrightarrow{k_{ec}} M + CO_2 + 2H^+ + 2e^- \tag{40}$$

$$CO_2 + 2(M\text{–}H) \xrightarrow{k_{rs}} M\text{–}CO + H_2O + M \tag{41}$$

CO adsorption and desorption were modeled by a Langmuir process. At steady state, the relationship between the anode polarization losses and the catalytic properties of the catalyst were investigated. The study further considered dilution and fuel utilization caused by reformate fuel containing CO_2. They concluded that the main effect of CO_2 poisoning is the blocking of the catalytic surface due to WGSR reaction. Subsequent desorption of CO from the catalyst surface, transport down the gas channel, and re-adsorption of CO play a minor role.

Zhang et al. [8] developed a kinetic model for a general PEM fuel cell anode contaminant. For a general contaminant P, the surface and electrochemical reactions at the anode can be described generally by the following reactions:

$$Pt + H_2 \underset{k_{1b}}{\overset{k_{1f}}{\longleftrightarrow}} Pt\text{–}H_2 \tag{42}$$

$$Pt\text{–}H_2 + Pt \underset{k_{2b}}{\overset{k_{2f}}{\longleftrightarrow}} 2Pt\text{–}H \tag{43}$$

$$Pt\text{–}H \underset{k_{3b}\ \exp[-(1-\alpha_3)n_3F\eta_a/RT]}{\overset{k_{3f}\ \exp[\alpha_3 n_3 F\eta_a/RT]}{\longleftrightarrow}} Pt + H^+ + e^- \tag{44}$$

$$\mathrm{P} + \mathrm{Pt} \underset{k_{4b}}{\overset{k_{4f}}{\longleftrightarrow}} \mathrm{Pt\text{–}P} \tag{45}$$

$$\mathrm{P} + \mathrm{Pt\text{–}H} \underset{k_{5b}\ \exp[-(1-\alpha_5)n_5 F\eta_a/RT]}{\overset{k_{5f}\ \exp[\alpha_5 n_5 F\eta_a/RT]}{\longleftrightarrow}} \mathrm{Pt\text{–}P} + \mathrm{H^+} + \mathrm{e^-} \tag{46}$$

$$\mathrm{P} + \mathrm{Pt\text{–}H_2} \underset{k_{6b}}{\overset{k_{6f}}{\longleftrightarrow}} \mathrm{Pt\text{–}P} + \mathrm{H_2} \tag{47}$$

$$\mathrm{Pt\text{–}P} + m\mathrm{H_2O} \underset{k_{7b}\ \exp[-(1-\alpha_7)qF\eta_a/RT]}{\overset{k_{7f}\ \exp[\alpha_7 qF\eta_a/RT]}{\longleftrightarrow}} \mathrm{Pt\text{–}P'} + q\mathrm{H^+} + q\mathrm{e^-} \tag{48}$$

$$\mathrm{Pt\text{–}P} + m\mathrm{H_2O} \underset{k_{8b}\ \exp[-(1-\alpha_8)qF\eta_a/RT]}{\overset{k_{8f}\ \exp[\alpha_8 qF\eta_a/RT]}{\longleftrightarrow}} \mathrm{Pt} + \mathrm{P'} + q\mathrm{H^+} + q\mathrm{e^-} \tag{49}$$

where P′ is the product of P electrochemical oxidation, $\alpha_{3,5,7,8}$ are electron transfer coefficients for individual electrochemical half-reactions, and η_a is anode overpotential.

The dissociation of adsorbed H_2 is considered to be the rate-determining step for hydrogen oxidation. The fast electrochemical oxidation of dissociated hydrogen atom (Reaction (44)) is believed to have a Nernst behaviour, from which the surface coverage of H_2, atomic H, and unoccupied Pt sites are derived as a function of contaminant surface coverage. The fuel cell current density expression as a function of anode and cathode overpotential were derived from the proposed reaction mechanism. Several characteristics such as performance loss, contamination transient time constant, and recovery were introduced to the model. The obtained equations were used to simulate contaminant coverage over time and recovery at different contaminant levels and current densities. These simulations demonstrated the model's ability for predicting performance recoverability.

5. Contamination mitigation

PEM fuel cells have been recognized as the most promising power sources for automobile applications due to zero emissions, high efficiency, and quiet operation. However, fuel cell contamination will become an issue due to fuel impurity and air pollution. As discussed above, the impurities in the hydrogen stream and pollutants in the air stream can contaminate the fuel cell MEA in many ways, causing performance degradation and failure. Therefore, the measures and methods for mitigation contamination have to be developed in order to minimize or eliminate its effects. In this section, the literature on the progress in contamination mitigation will be briefly reviewed. It seems that the majority of the literature deals with mitigation fuel-side contamination; only a few works focus on the cathode side.

For fuel, the reformed H_2-rich gas is the dominant source. As discussed above, this fuel contains appreciable amounts of CO and CO_2, which are the major fuel cell anode contaminants. There are several effective methods available to mitigate CO poisoning in PEM fuel cells, such as enhancing CO oxidation by pre-treating reformate, introducing an anode oxidant-bleed, developing CO-tolerant catalysts, and optimizing fuel cell operating conditions. Pre-treatment of reformate is one of the most popular ways to purify H_2-rich gas to reduce the CO concentration to as low as 10 ppm. Air or oxygen (or H_2O_2) bleeding has been demonstrated to be another effective way to reduce CO contamination if the fuel cell stack is operated with a reformate fuel stream. During fuel cell operation, air or oxygen will be intermittently blown into the anode. CO-tolerant catalyst development is another important mitigation method. As discussed above, the addition of a second or third metal into the Pt can form an alloying catalyst. The second or third metal can greatly help in CO oxidation. Operating a PEM fuel cell at high temperatures (>80 °C) has a significant benefit for contamination tolerance due to the weaker adsorption and faster oxidation rate of CO on the Pt catalyst. Zhang et al. [123] have comprehensively reviewed these points.

It is worthwhile to note that for a long-term supply of hydrogen, reformate may not be an option due to the fossil hydrogencarbon shortage. It is expected that the external supply of hydrogen will rely on electrolysis and reformate from renewable biomass materials such as methanol and ethanol. For H_2 production from water electrolysis, CO fuel contamination may not be a problem. However, for short-term hydrogen supplies, reformate is still an option in terms of cost and reliability.

For oxidant (air), the use of filters to purify the cathode feed stream effectively eliminated contamination from diesel and dust emission, hence improving the performance of a PEM fuel cell operated in an underground mine [124].

5.1. Fuel-side mitigation

5.1.1. Pre-treatment of reformate

The most straightforward method of mitigation is to purify the feed streams before they enter the fuel cell stack. Pre-treatment of reformate to obtain purer fuel serves that purpose. In the pre-treatment of reformate, purer hydrogen can be obtained using preferential or selective oxidation [125]. Alternatively, hydrogen purification can also be undertaken by combining a CO_2 scrubber with subsequent methanation to reduce CO content to a level of less than 10 ppm [126]. However, fuel cell power systems could become more complicated and expensive if the reformate is pre-treated on board.

5.1.2. Air- (or oxygen- or hydrogen peroxide-) bleeding techniques

Anode air- (or oxygen-) bleeding has been considered a preferable choice for CO contamination reduction due to its simplicity, effectiveness, and economic value. By blending low levels of an oxidant such as air, oxygen, or hydrogen peroxide into the anode fuel stream, the levels of CO from reformate can be reduced by the WGSR mechanism and selective oxidation of CO. It was reported that the deleterious effect on cell performance could be completely eliminated at 80 °C by injecting 4.5% air to a H_2/100 ppm CO anode feed stream [127], and up to 90% of the CO poisoning could be recovered in 1 min by bleeding 5% air to H_2/52.7 ppm CO fuel [128,129]. A 5% H_2O_2 in an anode humidifier could mitigate 100 ppm CO in a H_2-rich feed [130]. The mitigation mechanism for performance recovery by oxidant bleeding was discussed by Bellows et al. [131], who

demonstrated that even 0.75% H_2O_2 in the stainless steel humidifier could restore the cell performance even when an impure H_2 containing 96 ppm CO was used. However, this oxidant-bleeding method can cause overheating problems at the anode if the oxidant is not controlled and mixed properly. The reconfigured anodes could potentially enhance the effectiveness of air-bleed for CO-tolerance improvement (approaching 100 ppm) [132]. In this case, the GDL (carbon cloth) was modified to facilitate the effectiveness of oxidant-bleeding.

5.1.3. CO-tolerant electrocatalysts

As discussed above, developing contaminant-tolerant catalysts is a major area of focus for mitigation contamination in PEM fuel cells. To address this, alloying or co-depositing Pt with one or more other metals has been widely investigated with respect to CO-tolerant anode catalysts. The PtRu alloy catalysts, which have been commercially used in the PEM fuel cell industry, were shown to be the best CO-tolerant catalysts. Other unsupported or supported Pt-based alloy catalysts have also been demonstrated to exhibit high tolerance to CO poisoning. These include:

- Binary (PtM where M = Mo, Nb, Ta, Sn, Co, Ni, Fe, Cr, Ti, Mn, V, Zr, Pd, Os, Rh) [132–143].
- Ternary (PtRuM where M = Mo, Nb, Ta, Sn, Co, Ni, Fe, Cr, Ti, Mn, V, Zr, Pd, Os, Rh) [132–143].
- Quaternary ($PtRuM_1M_2$ where M = RuMoNb) [133–143].
- Pt-based metal oxide catalysts ($PtMO_x$ where M = W) [144] ($PtRuMO_x$ where M = Sn, W) [95,138].
- Pt-based composite-supported PtRu-H_xMO_3/C (where M = W, Mo) [145] and organic metal complexes [146].

More information on the development of high-performance and cost-effective CO-tolerant anode electrocatalysts for PEM fuel cells can be found in several comprehensive review articles [3,21,32,147–149].

In addition, improvements in catalyst preparation methods have been advanced considerably in order to better control particle-size distribution and the chemical composition of catalysts. CO tolerance can be significantly enhanced by Pt-based catalysts prepared by high energy ball-milling [150], sulfided (synthesized using $Na_2S_2O_3$) [151], and combustion synthesis [152]. A composite anode structure can also reduce CO poisoning. Placing a layer of carbon-supported Ru between the Pt catalyst layer and the anode flow field to form a Ru filter improved CO tolerance considerably [138], because the Ru layer supplied hydroxyl species to enhance CO oxidation.

Other anode configurations with dual-layer to three-layer electrodes were also explored to improve CO tolerance [153]. A bilayer anode with an extra inner layer adjacent to the backing for CO-oxidation promotion at low potential and an outer catalyst layer for fast H_2 oxidation [154,155], was shown to enhance CO/CO_2 tolerance. A novel composite anode has also effectively increased CO/CO_2 tolerance. It featured (1) an inner layer of a pure Pt produced by a direct-printing method onto the PEM; (2) an outer layer consisting of a nano Ru/Pt layer deposited by magnetron sputtering; and (3) a $Pt_{50}Ru_{50}$ layer applied by screen-printing on the GDL, which acts as CO "filter" [156].

5.1.4. High-temperature operation

High-temperature operation of PEM fuel cells has many advantages and can solve or avoid contamination problems [123]. As discussed above, CO poisoning effects are strongly temperature dependent. For example, when operating at high temperatures, CO tolerance was greatly improved from 10 to 20 ppm at 80 °C to 1000 ppm at 130 °C and 30,000 ppm at 200 °C [29]. The loading of the anode catalyst (PtRu) could be reduced from 0.40 to 0.20 $g_{PtRu}\,kW^{-1}$ at temperatures higher than 80 °C [157]. Therefore, at high temperatures it is possible to directly use reformate from a simple reformer as the feed fuel. The water gas shift reactor, selective oxidizer, and membrane separator for CO cleanup can be eliminated from the system, which yields a tremendous system cost savings. Other benefits of high-temperature operation include fast kinetics of hydrogen oxidation and oxygen reduction, as well as facile water management, which should also have a positive effect on contamination tolerance. The key issue in high-temperature operation is to develop alternative PEMs that can be operated at temperatures higher than 100 °C. Li et al. [158] reviewed approaches to PEMs operated at high temperatures (>100 °C) and suggested that acid–base polymer membranes, particularly H_3PO_4-doped polybenizimidazole (PBI), can be operated at temperatures up to 200 °C.

5.2. Air-side mitigation

Little information about cathode contamination mitigation is available from the literature. An air intake filter consisting of a balston filter and two quartz fibre filters in parallel was shown to significantly reduce insoluble dust and particle contamination under mine conditions with diesel emission gases, notably CO, CO_2, NO, NO_2, SO_2, and dust emissions [124].

6. Concluding remarks

Significant progress has been made in identifying fuel cell contamination sources and understanding the effects of contamination on performance through experimental, theoretical/modeling, and methodological approaches. It has been demonstrated that even trace amounts of impurities present in the fuel or air streams or fuel cell system components can severely poison the anode, membrane, and cathode, particularly at low-temperature operation. The contaminants can strongly or irreversibly adsorb on the catalyst surface to block the reaction sites, enter the membrane to reduce proton conductivity, and cross over the membrane to affect the other side of the MEA.

Fuel cell contamination and its effects on cell performance can be classified into three main categories: (1) poisoning of the electrode catalysts, resulting in kinetic effect, (2) reducing proton conductivities including those of the membrane and catalyst ionomer layers, and (3) degrading catalyst layer structure and hydrophobility, causing mass transfer problems.

CO, as a typical fuel contaminant, has been investigated most extensively through both experimental and theoretical approaches because at this stage of development, the H_2 source is reformate, in which CO is the major impurity. Several evaluation methods and theoretical models have been developed and verified for the CO poisoning mechanism. However, it is worthwhile to note that fossil reformate may not be a potential source of a long-term supply of hydrogen, because of future fossil hydrogencarbon shortages. Instead, it is expected that the external supply of hydrogen will rely on electrolysis and reformate from renewable biomass materials such as methanol and ethanol. For H_2 production from water electrolysis, CO fuel contamination may not be a problem. However, for short-term hydrogen supplies, reformate is still an option in terms of cost and reliability.

Other typical contaminants such as CO_2, sulfur-containing species (H_2S, and SO_x), NO_x, ammonia, and cationic ions have also been investigated. Their individual effects on fuel cell performance have been discussed extensively.

With respect to mitigation, most approaches have focused on the fuel side rather than on the cathode side. There are several effective methods to mitigate anode contamination, including pre-treatment of reformate, anode oxidant-bleeding, CO tolerant catalyst synthesis, and high-temperature operations. These methods have been developed to either minimize or eliminate CO contamination effects. The pre-treatment of reformate is straightforward but expensive, while the oxidant-bleeding method is simple and effective, but difficult to control. New catalyst synthesis methods for CO tolerance show promise, but cost is an issue. Although high-temperature operation of a PEM fuel cell is an effective way to reduce CO contamination, the membrane tolerance to high temperatures seems to be a limitation. Based on this literature survey, the developments in mitigation of other contaminants, especially those affecting cathode performance, have not been well documented.

On the path toward fuel cell commercialization, contamination prevention and mitigation must be addressed in order to facilitate research and development. The following approaches are suggested for future work:

(1) Air-side (or cathode) contamination studies with a focus on the fundamental understanding of contamination mechanisms, experimental validation, and mitigation strategies.
(2) Multi-contaminant effects on fuel cell performance with a focus on both the air and the fuel side. Theoretical modeling and validation will bring contamination research closer to practical operation situations.
(3) Contamination effects on fuel cell lifetime performance in conditions closer to practical operations, such as start/stop cycles, cold start-up, and dynamic loads.
(4) Fuel cell contamination prediction through contaminant sensing/monitoring, and theoretical/empirical modeling. For contaminant sensing/monitoring, *in situ* tools including sensors must be developed to report critical contaminant levels for performance prediction, and at the same time, to recognize contamination problems as early as possible. It is expected that the developed models validated by experimental data should be able to predict the performance drop if the contaminant levels and operation conditions are known.
(5) Contamination prevention and mitigation. Some measures must be developed to purify the feed streams and component materials. With respect to this, separate contaminant filters for fuel and air streams should be invented to filter out <0.005 ppm levels of contaminants; this is expected to be an extremely challenging aspect of this technology. On the other hand, it is also necessary to invent and develop contamination tolerance MEA components such as catalysts, catalyst layers and membranes.

Acknowledgements

We wish to thank the Institute for Fuel Cell Innovation, National Research Council Canada (NRC-IFCI) for its financial support. Discussions with Dr. Yoga Yogendran, Dr. Francois Girard, and Dr. Radenka Mirac from NRC-IFCI, Mr. Rajeev Vohra, Dr. Silvia Wessel, Mr. Nengyou Jia, and Ms. Shanna Knights from Ballard, and Mr. David Frank from Hydrogenics are highly appreciated. Dr. Xuan Cheng also greatly appreciates the financial supports from the China Scholarship Council and the National Natural Science Foundation of China (20433060).

References

[1] J. St-Pierre, D.P. Wilkinson, AIChE J. 47 (2001) 1482.
[2] D.L. Trimm, Z.I. Önsan, Catal. Rev. Sci. Eng. 43 (2001) 31.
[3] V.M. Vishnyakov, Vacuum 80 (2006) 1053.
[4] T.R. Ralph, Platinum Met. Rev. 43 (1999) 14.
[5] S.M. Park, T.J. O'Brien, Effects of several trace contaminants on fuel cell performance, Technical Report (# DOE/METC/RI-80/16), Department of Energy, Morgantown, WV, USA, 1980.
[6] P.R. Hayter, P. Mitchell, R.A.J. Dams, C. Dudfield, N. Gladding, The effect of contaminants in the fuel and air streams on the performance of a solid polymer fuel cell, Contract Report (ETSUF/02/00126/REP), Wellman CJB Limited, Portsmouth, UK, 1997.
[7] J. St-Pierre, D.P. Wilkinson, S. Knights, M. Bos, J. New Mater. Electrochem. Syst. 3 (2000) 99.
[8] J. Zhang, H. Wang, D.P. Wilkinson, D. Song, J. Shen, Z.S. Liu, J. Power Sources 147 (2005) 58.
[9] S. Knights, N. Jia, C. Chuy, J. Zhang, Fuel Cell Seminar 2005: Fuel Cell Progress, Challenges and Markets, Palm Springs, California, 2005.
[10] A.L. Dicks, J. Power Sources 61 (1996) 113.
[11] B. Hohlein, M. Boe, J. Bogild-Hansen, P. Brockerhoff, G. Colsman, B. Emonts, R. Menzer, E. Riedel, J. Power Sources 61 (1996) 143.
[12] V.M. Schmidt, P. Brockerhoff, B. Hohlein, R. Menzer, U. Stimming, J. Power Sources 49 (1994) 299.
[13] R. Parsons, T. VanderNoot, J. Electroanal. Chem. 257 (1988) 9.
[14] J.H. Wee, K.Y. Lee, S.H. Kim, Fuel Process. Technol. 87 (2006) 811.
[15] J.M. Moore, P.L. Adcock, J.B. Lakeman, G.O. Mepsted, J. Power Sources 85 (2000) 254.
[16] D. Yang, J. Ma, L. Xu, M. Wu, H. Wang, Electrochim. Acta 51 (2006) 4039.
[17] R. Mohtadi, W. Lee, J.W. Van Zee, J. Power Sources 138 (2004) 216.
[18] S.-Y. Ahn, S.-J. Shin, H.Y. Ha, S.-A. Hong, Y.-C. Lee, T.W. Lim, I.-H. Oh, J. Power Sources 106 (2002) 295.
[19] Joint Hydrogen Quality Task Force, USFCC Materials and Components Working Group, USFCC Transportation Working Group, US Fuel Cell Council, 2006.
[20] A. Collier, H. Wang, X. Zi Yuan, J. Zhang, D.P. Wilkinson, Int. J. Hydrogen Energy 31 (2006) 1838.
[21] J.J. Baschuk, X.G. Li, Int. J. Energy Res. 25 (2001) 695.

[22] A. Rodrigues, J.C. Amphlett, R.F. Mann, B.A. Peppley, P.R. Roberge, Proceedings of the Thirty Second Intersociety Energy Conversion Engineering Conference, 1997, p. 768.
[23] R.A. Lemons, J. Power Sources 29 (1990) 251.
[24] C.M. Seymour, J. Power Sources 37 (1992) 155.
[25] S. Jimenez, J. Soler, R.X. Valenzuela, L. Daza, J. Power Sources 151 (2005) 69.
[26] R. Benesch, T. Jacksier, 2005 IEEE Vehicle Power and Propulsion Conference, 2006, p. 481.
[27] J. Divisek, H.-F. Oetjen, V. Peinecke, V.M. Schmidt, U. Stimming, Electrochim. Acta 43 (1998) 3811.
[28] R. Jiang, H.R. Kunz, J.M. Fenton, J. Electrochem. Soc. 152 (2005) A1329–A1340.
[29] Q.F. Li, R.H. He, J.A. Gao, J.O. Jensen, N.J. Bjerrum, J. Electrochem. Soc. 150 (2003) A1599–A1605.
[30] M. Murthy, M. Esayian, W.K. Lee, J.W. Van Zee, J. Electrochem. Soc. 150 (2003) A29–A34.
[31] H.-F. Oetjen, V.M. Schmidt, U. Stimming, F. Trila, J. Electrochem. Soc. 143 (1996) 3838.
[32] T.R. Ralph, M.P. Hogarth, Platinum Met. Rev. 46 (2002) 117.
[33] L. Gubler, G.G. Scherer, A. Wokaun, Chem. Eng. Technol. 24 (2001) 59.
[34] A. Taniguchi, T. Akita, K. Yasuda, Y. Miyazaki, J. Power Sources 130 (2004) 42.
[35] T. Gu, W.-K. Lee, J.W. Van Zee, M. Murthy, J. Electrochem. Soc. 151 (2004) A2100–A2105.
[36] K.K. Bhatia, C.Y. Wang, Electrochim. Acta 49 (2004) 2333.
[37] T.E. Springer, T. Tockward, T.A. Zawodzinski, S. Gottesfeld, J. Electrochem. Soc. 148 (2001) A11–A23.
[38] Z. Qi, C. He, A. Kaufman, Electrochem. Solid-State Lett. 4 (2001) A204–A205.
[39] Z. Qi, C. He, A. Kaufman, J. Power Sources 111 (2002) 239.
[40] J.X. Zhang, T. Thampan, R. Datta, J. Electrochem. Soc. 149 (2002) A765–A772.
[41] J.D. Kim, Y.I. Park, K. Kobayashi, M. Nagai, J. Power Sources 103 (2001) 127.
[42] J.-N. Han, G.-G. Park, Y.-G. Yoon, T.-H. Yang, W.-Y. Lee, C.-S. Kim, Int. J. Hydrogen Energy 28 (2003) 609.
[43] W.-K. Lee, J.W. Van Zee, M. Murthy, Fuel Cells 3 (2003) 52.
[44] K. Narusawa, M. Hayashida, D. Kurashima, K. Wakabayashi, Y. Kamiya, JSME Int. J. Ser. B: Fluids Therm. Eng. 46 (2003) 643.
[45] K.W. Kirby, A.C. Chu, K.C. Fuller, Sens. Actuators B: Chem. 95 (2003) 224.
[46] R. Mukundan, E.L. Brosha, F.H. Garzon, Solid State Ionics 175 (2004) 497.
[47] J.M. Rheaume, B. Muller, M. Schulze, J. Power Sources 76 (1998) 60.
[48] K. Jambunathan, B.C. Shah, J.L. Hudson, A.C. Hillier, J. Electroanal. Chem. 500 (2001) 279.
[49] N. Wagner, E. Gulzow, J. Power Sources 127 (2004) 341.
[50] J.-D. Kim, Y.-I. Park, K. Kobayashi, M. Nagai, M. Kunimatsu, Solid State Ionics 140 (2001) 313.
[51] M. Ciureanu, H. Wang, J. Electrochem. Soc. 146 (1999) 4031.
[52] M. Ciureanu, H. Wang, J. New Mater. Electrochem. Syst. 3 (2000) 107.
[53] M.-C. Yang, C.-H. Hsueh, J. Electrochem. Soc. 153 (2006) A1043–A1048.
[54] M. Ciureanu, S.D. Mikhailenko, S. Kaliaguine, Catal. Today 82 (2003) 195.
[55] Y.J. Leng, X. Wang, I.M. Hsing, J. Electroanal. Chem. 528 (2002) 145.
[56] J.-M. Le Canut, R.M. Abouatallah, D.A. Harrington, J. Electrochem. Soc. 153 (2006) A857–A864.
[57] N. Rajalakshmi, T.T. Jayanth, K.S. Dhathathreyan, Fuel Cells 3 (2003) 177.
[58] F.A. de Bruijn, D.C. Papageorgopoulos, E.F. Sitters, G.J.M. Janssen, J. Power Sources 110 (2002) 117.
[59] G.J.M. Janssen, J. Power Sources 136 (2004) 45.
[60] T. Gu, W.K. Lee, J.W.V. Zee, Appl. Catal. B: Environ. 56 (2005) 43.
[61] D.C. Papageorgopoulos, F.A. de Bruijn, J. Electrochem. Soc. 142 (2002) A140–A145.
[62] T. Smolinka, M. Heinen, Y.X. Chen, Z. Jusys, W. Lehnert, R.J. Behm, Electrochim. Acta 50 (2005) 5189.
[63] R. Mohtadi, W.-K. Lee, S. Cowan, J.W. Van Zee, M. Murthy, Electrochem. Solid-State Lett. 6 (2003) A272–A274.
[64] M.J. Escudero, S. Jimenez, L. Daza, Proceedings of the 1st European Fuel Cell Technology and Applications Conference 2005, Book of Abstracts, vol. 2005, 2005, p. 169.
[65] R. Mohtadi, W.K. Lee, J.W. Van Zee, Appl. Catal. B: Environ. 56 (2005) 37.
[66] F. Laurencelle, R. Chahine, J. Hamelin, K. Agbossou, M. Fournier, T.K. Bose, A. Laperriere, Fuel Cells 1 (2001) 66.
[67] J. Kim, S.-M. Lee, S. Srinivasan, J. Electrochem. Soc. 142 (1995) 2670.
[68] J.C. Amphlett, R.M. Baumert, R.F. Mann, B.A. Peppley, P.R. Roberge, J. Electrochem. Soc. 142 (1995) 1.
[69] S. Srinivasan, E.A. Ticianelli, C.R. Derouin, A. Redondo, J. Power Sources 22 (1988) 359.
[70] F.A. Uribe, S. Gottesfeld Jr., T.A. Zawodzinski, J. Electrochem. Soc. 149 (2002) A293–A296.
[71] R. Halseid, P.J.S. Vie, R. Tunold, J. Power Sources 154 (2006) 343.
[72] H.J. Soto, W.-K. Lee, J.W. Van Zee, M. Murthy, Electrochem. Solid-State Lett. 6 (2003) A133–A135.
[73] R. Halseid, P.J.S. Vie, R. Tunold, J. Electrochem. Soc. 151 (2004) A381–A388.
[74] H.L. Yeager, A. Steck, J. Electrochem. Soc. 128 (1981) 1880.
[75] M.J. Kelly, B. Egger, G. Fafilek, J.O. Besenhard, H. Kronberger, G.E. Nauer, Solid State Ionics 176 (2005) 2111.
[76] M. Shi, F.C. Anson, J. Electroanal. Chem. 425 (1997) 117.
[77] Z. Samec, A. Trojanek, J. Langmaier, E. Samcova, J. Electrochem. Soc. 144 (1997) 4236.
[78] M. Inaba, T. Kinumoto, M. Kiriake, R. Umebayashi, A. Tasaka, Z. Ogumi, Electrochim. Acta 51 (2006) 5746.
[79] G. Pourcelly, A. Oikonomou, C. Gavach, H.D. Hurwitz, J. Electroanal. Chem. 287 (1990) 43.
[80] T. Okada, N. Nakamura, M. Yuasa, I. Sekine, J. Electrochem. Soc. 144 (2006) 2744.
[81] T. Okada, S. Moller-Holst, O. Gorseth, S. Kjelstrup, J. Electroanal. Chem. 442 (1998) 137.
[82] G. Xie, T. Okada, J. Electrochem. Soc. 142 (1995) 3057.
[83] A. Pozio, R.F. Silva, M. De Francesco, L. Giorgi, Electrochim. Acta 48 (2003) 1543.
[84] M.J. Kelly, G. Fafilek, J.O. Besenhard, H. Kronberger, G.E. Nauer, J. Power Sources 145 (2005) 249.
[85] M. Boillot, C. Bonnet, N. Jatroudakis, P. Carre, S. Didierjean, F. Lapicque, Fuel Cells 6 (2006) 31.
[86] P. Stonehart, P.N. Ross, Catal. Rev.-Sci. Eng. 12 (1975) 1.
[87] M. Watanabe, S. Motoo, J. Electroanal. Chem. 206 (1986) 197.
[88] H. Igarashi, T. Fujino, M. Watanabe, J. Electroanal. Chem. 391 (1995) 119.
[89] H.A. Gasteiger, N.M. Markovic Jr., P.N. Ross, E.J. Cairns, J. Phys. Chem. 98 (1994) 617.
[90] H.A. Gasteiger, N.M. Markovic Jr., P.N. Ross, J. Phys. Chem. 99 (1995) 16757.
[91] T.J. Schmidt, H.A. Gasteiger, R.J. Behm, J. Electrochem. Soc. 146 (1999) 1296.
[92] R. Ianniello, V.M. Schmidt, J.L. Rodriguez, E. Pastor, J. Electroanal. Chem. 471 (1999) 167.
[93] F. Buatier de Mongeot, M. Scherer, B. Gleich, E. Kopatzki, R.J. Behm, Surf. Sci. 411 (1998) 249.
[94] L. Giorgi, A. Pozio, C. Bracchini, R. Giorgi, S. Turt, J. Appl. Electrochem. V31 (2001) 325.
[95] S.J. Copper, A.G. Gunner, G. Hoogers, D. Thompsett, Proceedings of the Second International Symposium on New Materials for Fuel Cell and Modern Battery Systems II, 1997, p. 286.
[96] E. Christoffersen, P. Liu, A. Ruban, H.L. Skriver, J.K. Norskov, J. Catal. 199 (2001) 123.
[97] S. Gilman, J. Phys. Chem. 68 (1964) 70.
[98] M.C. Arevalo, C. Gomis-Bas, F. Hahn, B. Beden, A. Arevalo, A.J. Arvia, Electrochim. Acta 39 (1994) 793.

[99] S. Taguchi, T. Ohmori, A. Aramata, M. Enyo, J. Electroanal. Chem. 369 (1994) 199.
[100] B.Z. Nikolic, H. Huang, D. Gervasio, A. Lin, C. Fierro, R.R. Adzic, E. Yeager, J. Electroanal. Chem. 295 (1990) 415.
[101] H. Huang, C. Fierro, D. Scherson, E.B. Yeager, Langmuir 7 (1991) 1154.
[102] B. Beden, A. Bewick, M. Razaq, J. Weber, J. Electroanal. Chem. 139 (1982) 203.
[103] T. Iwasita, F.C. Nart, B. Lopez, W. Vielstich, Electrochim. Acta 37 (1992) 2361.
[104] J. Giner, Electrochim. Acta 8 (1963) 857.
[105] A. Czerwinski, J. Sobkowski, A. Wieckowski, Int. J. Appl. Radiat. Isotopes 25 (1974) 295.
[106] J. Sobkowski, A. Czerwinski, J. Electroanal. Chem. 55 (1974) 391.
[107] J. Sobkowski, A. Czerwinski, J. Electroanal. Chem. 65 (1975) 327.
[108] J. Sobkowski, A. Czerwinski, J. Phys. Chem. 89 (1985) 365.
[109] M.V. Mathieu, M. Primet, Appl. Catal. 9 (1984) 361.
[110] N. Ramasubramanian, J. Electroanal. Chem. 64 (1975) 21.
[111] A. Michaelides, P. Hu, J. Chem. Phys. 115 (2001) 8570.
[112] A.Q. Contractor, H. Lal, J. Electroanal. Chem. 96 (1979) 175.
[113] T. Loucka, J. Electroanal. Chem. 31 (1971) 319.
[114] A.Q. Contractor, H. Lal, J. Electroanal. Chem. 93 (1978) 99.
[115] T. Okada, G. Xie, Y. Tanabe, J. Electroanal. Chem. 413 (1996) 49.
[116] X. Wang, I.M. Hsing, Y.J. Leng, P.L. Yue, Electrochim. Acta 46 (2001) 4397.
[117] T. Springer, T. Zawodzinski, S. Gottesfeld, in: J. McBreen, S. Mukherjee, S. Srinivasan (Eds.), Electrode Material and Processes for Energy Conversion and Storage IV, Pennington, NJ, 1997, p. 15.
[118] P. Rama, R. Chen, R. Thring, Proc. Inst. Mech. Eng. Part A: J. Power Energy 219 (2005) 255.
[119] K.K. Bhatia, C.-Y. Wang, Electrochim. Acta 49 (2004) 2333.
[120] J.J. Baschuk, A.M. Rowe, X.G. Li, Trans. ASME J. Energy Resour. Technol. 125 (2003) 94.
[121] J.J. Baschuk, X. Li, Int. J. Global Energy Issues 20 (2003) 245.
[122] S.H. Chan, S.K. Goh, S.P. Jiang, Electrochim. Acta 48 (2003) 1905.
[123] J. Zhang, Z. Xie, J. Zhang, Y. Tang, C. Song, T. Navessin, Z. Shi, D. Song, H. Wang, D.P. Wilkinson, J. Power Sources 160 (2006) 872.
[124] M.C. Betournay, G. Bonnell, E. Edwardson, D. Paktunc, A. Kaufman, A.T. Lomma, J. Power Sources 134 (2004) 80.
[125] T.V. Choudhary, D.W. Goodman, Catal. Today 77 (2002) 65.
[126] K. Ledjeff-Hey, J. Roes, R. Wolters, J. Power Sources 86 (2000) 556.
[127] S. Gottesfeld, J. Pafford, J. Electrochem. Soc. 135 (1988) 2651.
[128] C.-C. Chung, C.-C. Hsun, L.-H. Hui, Y.-Y. Yie, Proceedings of the 3rd International Conference on Fuel Cell Science, Engineering, and Technology, 2005, p. 215.
[129] L.Y. Sung, Y.Y. Yan, H.S. Chu, R.J. Shyu, F. Chen, Proceedings of the 2nd International Conference on Fuel Cell Science, Engineering, and Technology, 2004, p. 621.
[130] V.M. Schmidt, H.-F. Oetjen, J. Divisek, J. Electrochem. Soc. 144 (1997) L237–L238.
[131] R.J. Bellows, E. Marucchi-Soos, R.P. Reynolds, Electrochem. Solid-State Lett. 1 (1998) 69.
[132] P.A. Adcock, S.V. Pacheco, K.M. Norman, F.A. Uribe, J. Electrochem. Soc. 152 (2005) A459–A466.
[133] F. Lufrano, E. Passalacqua, G. Squadrito, A. Patti, Proceedings of the HYPOTHESES-II-Symposium, 1998, p. 591.
[134] M. Gotz, H. Wendt, Electrochim. Acta 43 (1998) 3637.
[135] G.L. Holleck, D.M. Pasquariello, S.L. Clauson, Proceedings of the Second International Symposium on Proton-Conducting Membrane Fuel Cells II, 1999, p. 150.
[136] D.C. Papageorgopoulos, M. Keijzer, J.B.J. Veldhuis, F.A. de Bruijn, J. Electrochem. Soc. 149 (2002) A1400–A1404.
[137] G. Garcia, J.A. Silva-Chong, O. Guillen-Villafuerte, J.L. Rodriguez, E.R. Gonzalez, E. Pastor, Catal. Today 116 (2006) 415.
[138] C. He, R.V. Venkataraman, H.R. Kunz, J.M. Fenton, Hazardous and Industrial Wastes Proceedings of the Mid Atlantic Inductrial Waste Conference, 1999, p. 663.
[139] S. Mukerjee, R.C. Urian, S.J. Lee, E.A. Ticianelli, J. McBreen, J. Electrochem. Soc. 151 (2006) A1094–A1103.
[140] E.I. Santiago, M.S. Batista, E.M. Assaf, E.A. Ticianelli, J. Electrochem. Soc. 151 (2004) A944–A949.
[141] M. Iwase, S. Kawatsu, Proceedings of the First International Symposium on Proton Conducting Membrane Fuel Cells, vol. 1, 1995, p. 12.
[142] Y. Liang, H. Zhang, H. Zhong, X. Zhu, Z. Tian, D. Xu, B. Yi, J. Catal. 238 (2006) 468.
[143] D.C. Papageorgopoulos, M. Keijzer, F.A. de Bruijn, Electrochim. Acta 48 (2002) 197.
[144] L.G. Pereira, F.R. dos Santos, M.E. Pereira, V.A. Paganin, E.A. Ticianelli, Electrochim. Acta 51 (2006) 4061.
[145] Z. Hou, B. Yi, H. Yu, Z. Lin, H. Zhang, J. Power Sources 123 (2003) 116.
[146] H. Yano, C. Ono, H. Shiroishi, T. Okada, Chem. Commun. (2005) 1212.
[147] E. Antolini, Mater. Chem. Phys. 78 (2003) 563.
[148] J.H. Wee, K.Y. Lee, J. Power Sources 157 (2006) 128.
[149] N.P. Brandon, S. Skinner, B.C.H. Steele, Annu. Rev. Mater. Res. 33 (2003) 183.
[150] M.C. Denis, G. Lalande, D. Guay, J.P. Dodelet, R. Schulz, J. Appl. Electrochem. V29 (1999) 951.
[151] R. Venkataraman, H.R. Kunz, J.M. Fenton, J. Electrochem. Soc. 151 (2004) A710–A715.
[152] E. Chinarrom, B. Moreno, G.C. Mather, J.R. Jurado, J. New Mater. Electrochem. Syst. 7 (2004) 109.
[153] E. Antolini, J. Appl. Electrochem. V34 (2004) 563.
[154] G.J.M. Janssen, M.P. de Heer, D.C. Papageorgopoulos, Fuel Cells 4 (2004) 169.
[155] H. Yu, Z. Hou, B. Yi, Z. Lin, J. Power Sources 105 (2002) 52.
[156] C.H. Wan, Q.H. Zhuang, C.H. Lin, M.T. Lin, C. Shih, J. Power Sources 162 (2006) 41.
[157] H.A. Gasteiger, J.E. Panels, S.G. Yan, J. Power Sources 127 (2004) 162.
[158] Q. Li, R. He, J.O. Jensen, N.J. Bjerrum, Chem. Mater. 15 (2003) 4896.